The Local Impact of Climate Change on Air Quality

Report to DEFRA

by

Cambridge Environmental Research Consultants

and

The Met Office

25 October 2005

Report information

CERC Job Number:	FM642
Job Title:	The Local Impact of Climate Change on Air Quality
Prepared for:	DEFRA/CPEA22
Report Status:	Draft 3
Report Reference:	FM642/R

Author(s): David Carruthers, Kate Johnson, Sofia Girnary and Nicki Trought, CERC
Maria Athanassiadou, Jonathan Baker, William Collins, Colin Johnson, David Hassell, Matthew Hort, David Thomson and Claire Witham, Met Office

Other contributors:

Issue	Date	Comments
1	31/03/05	DRAFT
2	06/07/05	DRAFT 2
3	25/10/05	DRAFT 3

Contents

SUMMARY

The possible effects of climate change on air quality have been studied using meteorological data obtained from climate change simulations together with models for dispersion and atmospheric chemistry.

Meteorology from climate change simulations conducted by the Met Office has been extracted for London and Glasgow. This has been used to estimate the impact of climate change on air quality in these two urban areas, using CERC's statistical 'rural predictor' model to represent the regional background concentrations and CERC's ADMS-Urban model to represent the urban scale dispersion and chemistry. Estimates of regional background ozone concentrations have also been made using the Met Office's global chemical transport model STOCHEM.

The climate change simulations have been used to predict changes between the current climate and a future climate in the period ~2070-2090. The most obvious impact of climate change is on temperature where increases of order 2-4 ^{0}C are predicted. Temperature is a significant parameter for air pollution because of its effect, particularly in summer, on emission of biogenic ozone precursors and its influence on chemical reaction rates. Smaller and less clearly significant changes in other parameters are predicted as follows:

- An increase in wind speed in winter and reduction in summer.
- A tendency in London for more westerlies in winter and a shift from south-westerlies to north-westerlies in summer. Also a tendency in Glasgow for wind directions to become much more concentrated in the WSW direction.
- A small reduction in cloud cover in summer and a modest consequential increase in incoming solar radiation and surface heat flux.
- A modest increase in mean boundary layer depth in London (~50m) and a very small mean increase in Glasgow (~10m). .
- A decrease in precipitation in summer and an increase in winter.
- An increase in mean sea level pressure in summer and a decrease in winter, suggesting an increase in blocking circulation patterns in summer and in mobile westerly patterns in winter.
- An increase in specific humidity.

Dispersion predictions were made for a variety of single sources: a small source with a low stack, a small power station, a large power station and a road source. With the London met data, only the large power station showed significant differences, with a 13% increase in the spatial maxima of the annual average and the 98th percentile concentrations by ~2080. For Glasgow the effects were larger with increases in the range 25-39% for the annual average for all three non-road sources and for the 98th percentile for the power station source.

Predictions for long term average background concentrations of NO_x, NO_2, ozone and PM_{10} upwind of London and Glasgow were made using the 'rural predictor' model. This showed a 4.3 ppb fall in NO_x and a 5.1 ppb increase in ozone for London, while a 0.6 ppb fall in NO_2 was the largest predicted percentage change (-11%) for Glasgow (again by about 2080). Other changes were small. Predictions of background ozone

were also made with the STOCHEM model, giving increases of 6 ppb in long term average ozone, with similar values at both London and Glasgow. Although the rural predictor and STOCHEM give similar values for ozone (at least in London), it should be noted that (i) the rural predictor does not account for the projected increase in anthropogenic emissions, and (ii) the version of STOCHEM used here does not account for the likely increase with temperature of natural biogenic hydrocarbon emissions. It seems possible that a model that includes both these aspects will result in higher ozone predictions. STOCHEM predicts larger increases in peak monthly mean concentrations of ozone, with the worst months having concentrations above 60 ppb.

With the aid of the background estimates from the rural predictor, long term average concentrations of NO_x, NO_2, ozone and PM_{10} were estimated within the two urban areas. For London the results averaged over a number of sites show a fall in NO_x of 6.1 ppb and a rise in ozone of 4.0 ppb with only small changes in NO_2 and PM_{10}. For Glasgow, the changes in all four chemical species are small. Bigger changes are seen at individual sites, e.g. a fall of 11.5 ppb in NO_x at Marylebone Road and an increase of 5.1 ppb in ozone at Brent.

There are a number of potential implications for policy. The increases in impacts seen for some of the single sources imply that climate change may be important in the regulation of large sources. Also the impact of climate change on both rural and urban ozone may well be significant with increases in long term means of order 5 ppb. Peak increases could be substantially higher and would be expected to produce more frequent exceedances of ozone directives and standards. Also of significance is the fact that in London average NO_2 concentrations remain approximately constant despite reductions in NO_x. This results from greater availability of ozone and shows that projections of NO_2 based only on reductions in NO_x may underestimate NO_2.

It must be appreciated that there are many uncertainties in these results. Many aspects of climate change science are uncertain and so there are significant uncertainties in the predicted changes in meteorology. Results for temperature and winter precipitation are likely to be the most reliable with some degree of consensus between different models, while, at the other extreme, results for detailed boundary layer properties such as heat flux and boundary layer depth should be regarded as indicative only. There are also uncertainties in predicting the rural background concentrations from the meteorology – for example the extent to which the rural predictor model is valid in a changed climate and the extent to which the STOCHEM model results would change if temperature-sensitive biogenic emissions were included. Uncertainties will be increased further for the short term means which are used in many air quality standards. None-the-less, this study has shown there is a likelihood of significant changes in air quality due to climate change which deserves further investigation.

The Local Impact of Climate Change on Air Quality

1. Introduction

The links between air quality and climate change are currently generating great interest. For instance such links are being reviewed by DEFRA's air quality expert group (AQEG). One of a number of topic areas requested from AQEG by DEFRA is the impact of climate change on air quality. It is aspects of this topic which are addressed in this study, with the emphasis on the local, urban and regional scales. We note that there are a number of previous studies which have shown that climate change is likely to have an effect on aspects of air pollution (see e.g. Mickley et al., 2004, Langner et al., 2005 and Dentener at al., 2005).

There are two specific components to the study. Firstly the Met Office has used its climate models to simulate regional meteorology for the present climate and for a global-warming-affected future climate, and has derived datasets giving predictions of changes to local meteorological conditions. These datasets have been analysed to look at statistics of meteorological conditions in general and also those conducive to air pollution episodes. This analysis has been used to make a qualitative assessment of features of climate change likely to have an impact on air quality.

Secondly CERC has used the meteorological datasets as input to air dispersion calculations in order to estimate changes to air pollution impacts at a local scale, firstly looking at the local impact due to single point and road sources and then looking at the potential impact on urban pollution, considering both impacts on background pollution and local dispersion effects. Some regional scale background pollution predictions from the Met Office's global chemical transport model STOCHEM are also presented to complement the background predictions from CERC's 'rural predictor' model.

The analysis is carried out for two locations, London and Glasgow. The use of just two locations keeps the cost of the study limited while the choice of London and Glasgow, with their significantly different climates, provides some, albeit limited, information on variability across the UK.

Section 2 outlines the derivation of the climate change scenario, as conducted by the Met Office, and presents an analysis of the changes in the local climate for London and Glasgow. The results of CERC's dispersion modelling are given in Section 3 together with predictions from the STOCHEM model. Conclusions are presented in Section 4 and references given in Section 5.

2. Impacts of Climate Change on Local Meteorology

2.1 Generation of the climate change scenario

The climate change scenario was generated using the third-generation Hadley Centre regional climate model (HadRM3H) described by Hudson and Jones (2002b). This is the same model used in the UK Climate Impacts Programme (UKCIP) study conducted in 2002 (Hulme et al., 2002) and is closely related to the regional climate model HadRM3P used in the PRECIS (Providing Regional Climates for Impact Studies) modelling system (Jones et al., 2004). The model has 19 vertical levels in the atmosphere (from the surface to 30km in the stratosphere) and 4 levels in the soil and was run here with a horizontal resolution of 25km. It is a comprehensive physical model of the atmosphere and land surface, containing the same important processes in the climate system (e.g. clouds, radiation, rainfall, atmospheric sulphur cycle, soil hydrology) as are found in a global climate model. At its lateral boundaries, the regional climate model is driven by atmospheric winds, temperatures and humidity and aerosol particle concentration output from a global climate model.

There are many potential advantages of using a high resolution regional climate model rather than running a global climate model directly. These include a more realistic simulation of the current climate, prediction of climate change with more detail and with regional differences, explicit or better representation of islands which are smaller than or close to grid scale in global climate models, and better simulation and prediction of changes to extremes of weather (see Giorgi and Mearns, 1999, Lowe et al., 2001 and Frei et al., 2003, for some examples).

The climate simulations used here were originally carried out for the British-Irish Council (Jenkins et al., 2003). The experimental design was as follows. The third generation Hadley Centre coupled atmosphere-ocean climate model, HadCM3 (Gordon et al., 2000), was used to simulate climate change over the period 1861-1990 (driven by observed concentrations of greenhouse gases and estimates of sulphate aerosols), and a prediction was made for the period 1990-2100 driven by the A2 emission scenario of the SRES emissions scenarios (Nakićenović et al., 2000). The resolution of the atmosphere of HadCM3 is 2.5 degrees latitude by 3.75 degrees longitude, corresponding to ~300km over the UK. This relatively coarse resolution (in common with other global coupled models) limits the simulation of current climatic features, such as the statistics of Atlantic storm tracks, which have an important influence over UK.

In order to improve this, the predicted changes in sea surface temperatures and sea ice extent were input into a global atmosphere-only model, HadAM3H (Hudson and Jones, 2002a), having twice the horizontal resolution of the global coupled model; this gave a better representation of the storm tracks and other features. The HadAM3H model was run to simulate two 30-year periods, 1961-1990 (the most recent reference period of the WMO, representing recent climate) and 2071-2100.

The global simulations and predictions from the two HadAM3H model runs were downscaled to ~25km resolution (0.22 x 0.22 degrees) using the regional climate model HadRM3H giving high resolution results for the two periods 1961-1990 and 2071-2100. HadRM3H has the same physical and dynamical formulation as the driving global model (HadAM3H) except where resolution dependent parameter changes were required for stability, or where implied by the nature of the model's physical parameterizations. Despite the high spatial resolution of the model, the land use information used by the model is only resolved on a 1 degree grid. As a result there is no explicit representation of urban effects within the model. The area covered by the high resolution simulation is defined in a rotated latitude-longitude coordinate system (i.e. a system with the coordinate pole not at the true pole) and is shown, projected onto the normal latitude-longitude coordinate system, in Figure 1.

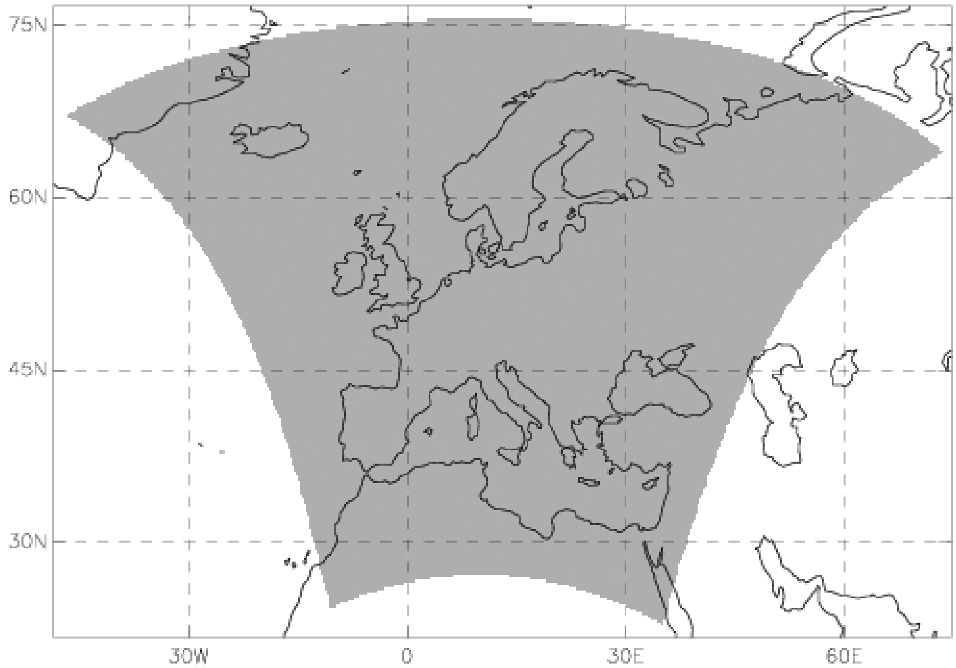

Figure 1: Area covered by the high resolution climate simulations conducted using HadRM3H.

We should point out that these simulations reflect the climate change resulting from just one possible emission scenario, namely the SRES A2 scenario. This corresponds to the 'medium-high' emissions scenario considered in the UKCIP02 report (Hulme et al., 2002). In addition the simulation does not provide any information on uncertainty due to the chaotic nature of the climate system (repeated runs of the model with similar but not identical initial conditions will give different results) or to 'scientific uncertainty' (different models will give different results depending both on the details of their formulation and the processes included). As a result our results should be regarded as no more than indicative of a possible future scenario. This is especially so for some of the more detailed boundary layer properties which are important for pollution dispersion. It is not possible to address these issues in any detail in this short report – for a detailed discussion of uncertainty in prediction of the future climate of the UK we refer the reader to Hulme et al. (2002). However we note that although the various emission scenarios lead to substantial differences in predictions for the end of the 21st century, the differences are much smaller for the first half of the century. This is partly because much of the climate change over the next few decades is determined by historic emissions and partly because, although the different scenarios have different predictions for greenhouse gases and sulphate aerosol concentrations, the differences in greenhouse gases are partly counteracted by the differences in sulphate.

A brief comparison of these 25km resolution simulations with the 50 km simulations presented in the UKCIP report by Hulme et al. (2002) was carried out by Buonomo et al. (2003). This focused mainly on temperature and precipitation changes and concluded that, when results were aggregated onto a 50 km grid, the differences were small except in coastal and mountainous areas. This is to be expected as it is in mountainous and coastal areas that conditions change most rapidly in space and where one would expect the improved resolution to have the biggest impact.

2.2 Analysis of the meteorological data from the climate simulations

Datasets containing hourly data for London and Glasgow were produced from the regional climate model simulation for the years 1971, 1976, 1981 and 1986 representing the current climate, and for 2071, 2076, 2081 and 2086, representing the future climate. Four years is not many over which to sample the climate, but by spacing the years we have made an attempt to sample variability on decadal time scales as well as year to year variability. The data are representative of the hour in question and so are time stamped on the half hour (00:30am, 01:30am etc). The London and Glasgow data are extracted at the nearest model grid points to the locations 0.1333W, 51.5N and 4.25E, 55.85N respectively. The high resolution of the simulations means there is little to be gained by spatial interpolation between grid points.

The datasets have been analysed to identify the differences between the two climates, with an emphasis on parameters which may have a significant effect on air pollution. The meteorology can affect air pollution in a number of ways, through changes in emissions (e.g. emissions associated with heating or natural emissions such as isoprene from vegetation, both of which have a strong temperature dependence), through changes in the transport and dispersion, through changes in atmospheric chemistry, and through changes in deposition. The main meteorological parameters selected for the analysis are listed here, along with a brief description of how they influence air quality:

- Wind speed – influences the stability of the atmospheric boundary layer and hence the dispersion as well as the dilution of pollution at its source.
- Wind direction – determines where pollutants are transported, in particular whether polluted continental air or clean Atlantic air dominates the transport to the UK.
- Cloud cover – influences stability of the atmospheric boundary layer through its effect on incoming solar radiation and surface heat flux.
- Incoming solar radiation – influences the stability of the atmospheric boundary layer though its effect on surface heat flux and drives photochemical reactions (i.e. ozone production).
- Surface heat flux – influences the stability of the atmospheric boundary layer.
- Boundary layer depth – determines the depth of atmosphere for pollutants to mix in (a low boundary layer will cause pollutants to be concentrated close to the ground).
- Temperature – influences man-made and biogenic emissions and chemical reaction rates.

- Precipitation – removes pollutants from the atmosphere.
- Pressure (mean sea level) – indicative of type of atmospheric circulation pattern which is related to other variables (e.g. wind speed, cloud cover, stability above the boundary layer, boundary layer depth etc).
- Specific humidity – plays a role in the chemical reactions occurring in the atmosphere.

Note that by stability we have in mind some measure of the relative importance of mechanical and thermal effects (e.g. Pasquill stability category, Monin-Obukhov length or Richardson number), and not just a measure of the thermal stratification.

The data was analysed to determine the frequency distribution of the above variables. Categories were defined for each parameter by introducing bands that split the data into a manageable number of groups. For example, temperature data was split into 2ºC bands. For each parameter, the fraction of hours that had data in each category was determined for each year, and this was then expressed as a percentage. This procedure was carried out four times, using all the data, using the summer data only (with summer defined here as April to September inclusive), using summer midday data only (12:30pm), and using winter data only (October to March inclusive). The summer midday data should give an idea of maximum surface heat flux and incoming solar radiation, although not of temperature or boundary layer depth. The results are presented graphically below. In each case the average for the four "current climate" years and for the four "future climate" years is plotted, together with error bars indicating the range occupied by the different years.

2.2(i) Results for London

In this section we present the results for London. Figures 2 and 3 show results for wind speed and direction. When all the data are considered, the effects of climate change are small. There is a small increase in speed, with a small increase in the frequency of westerlies and a corresponding decrease in the frequency of easterlies. However bigger differences are seen when summer and winter are considered separately. In summer, climate change is predicted to have the effect of generally reducing wind speeds, with reduced frequency of south-westerlies and increased frequency of north-westerlies. During the winter, the opposite is true for wind speed, with the results suggesting wind speeds will be on average greater in the future. There is also an increase in westerlies (south-westerlies in particular) and a reduction in easterlies. These changes are broadly consistent with those reported by Hulme et al. (2002) from a 50km grid HadRM3 simulation, but are not large and, as noted by Hulme et al., should not be regarded as very reliable because wind predictions differ significantly between different climate models. In comparing with the figures giving the change in surface pressure patterns in Hulme et al. (2002, Figure 82) it should be remembered that the surface wind tends to be backed relative to the geostrophic wind implied by the pressure patterns.

Wind roses for each of the years analysed are shown in Figure 4 while Figure 5 shows a wind rose combining all four past years, a wind rose combining all four future years, plus wind roses of summer and winter conditions. The differences between the past and future climate are consistent with those noted above in connection with Figures 2 and 3, but are not dramatic, being of the same order as the year to year variability.

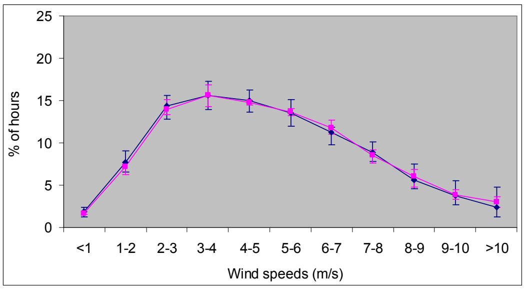

All data

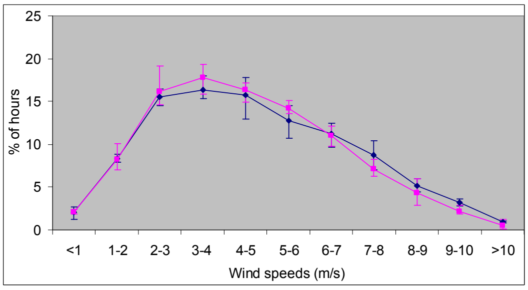

Summer data

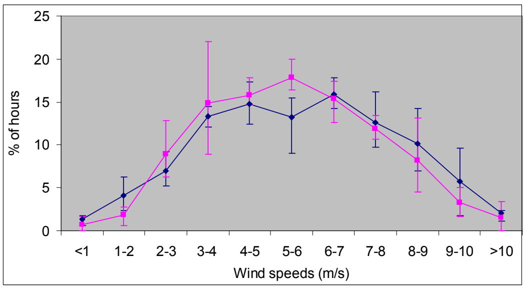

Summer midday data

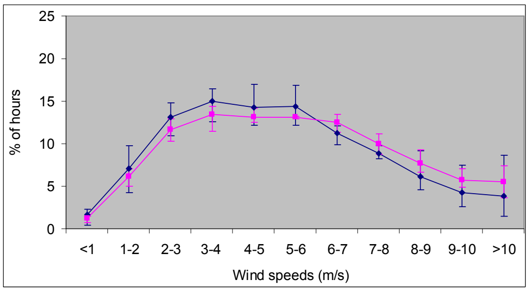

Winter data

Figure 2: Frequency distribution (%) of wind speeds (m/s) under current and future climate scenarios for London: —◆— Current —■— Future (note that here, and in all similar figures, the error bars give the entire range spanned by the four contributing years and not the standard deviation over the four years).

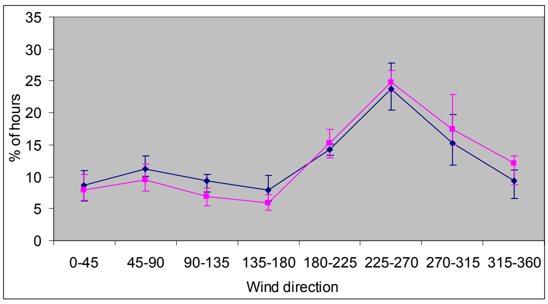

All data

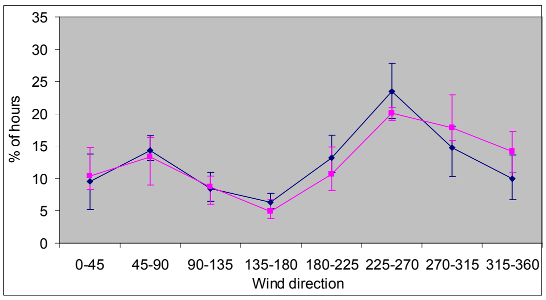

Summer data

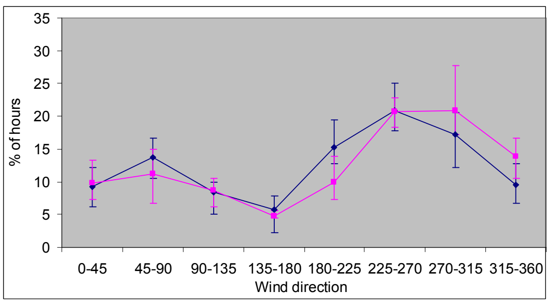

Summer midday data

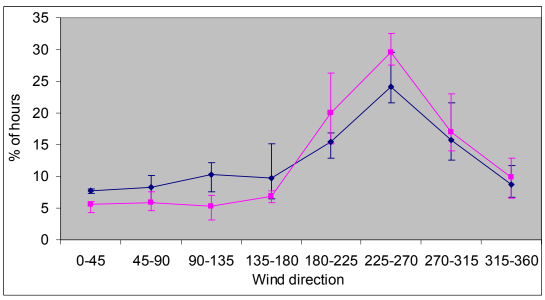

Winter data

Figure 3: Frequency distribution (%) of wind direction (^{0}) under current and future climate scenarios for London: —◆— Current —■— Future

Figure 4: Wind roses for London under the current and future climate scenarios, given separately for each of the years considered.

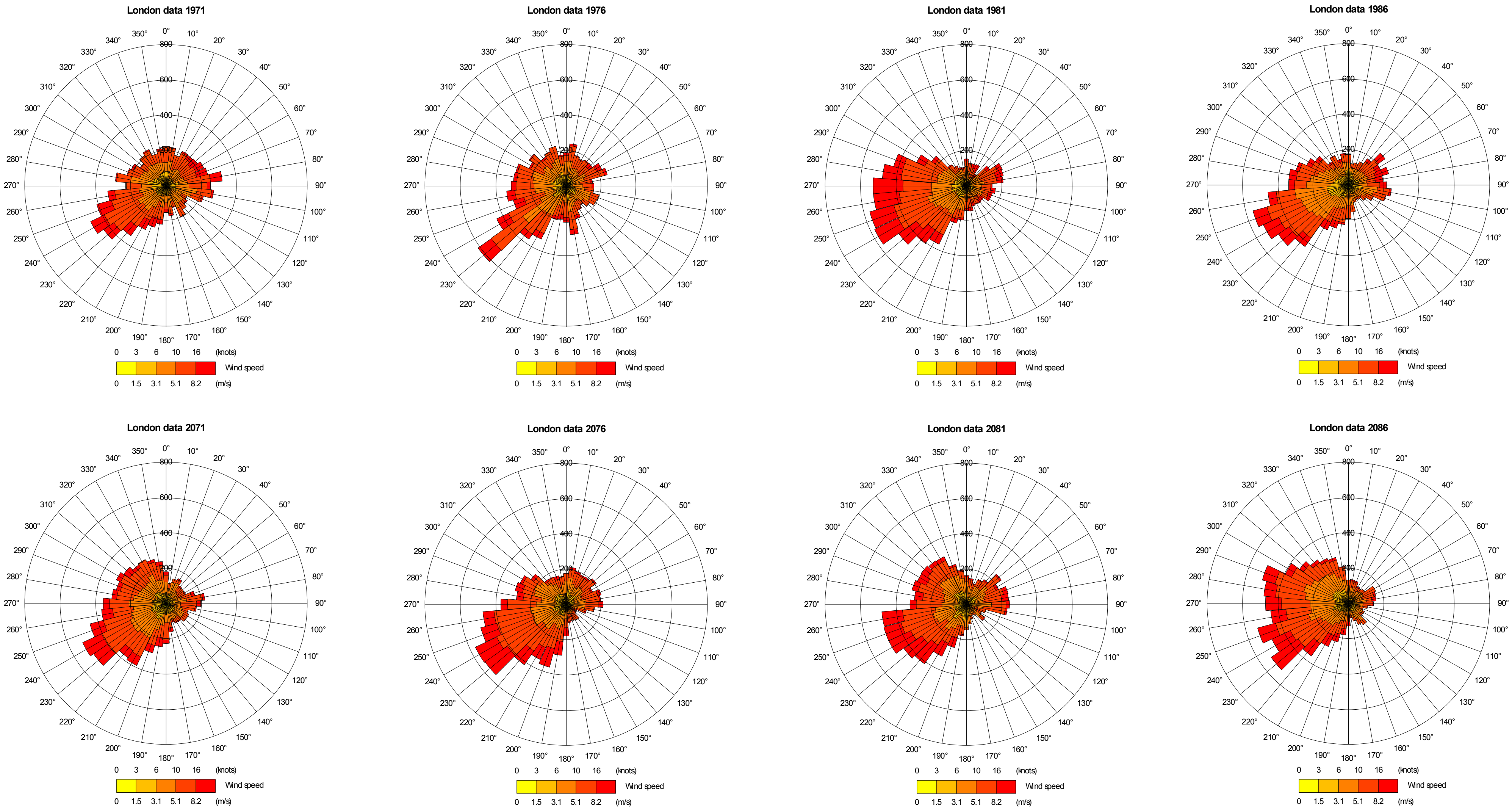

Figure 5: Wind roses for London under the current and future climate scenarios. All year, summer, and winter roses are presented. For each scenario, the results are for the four years combined.

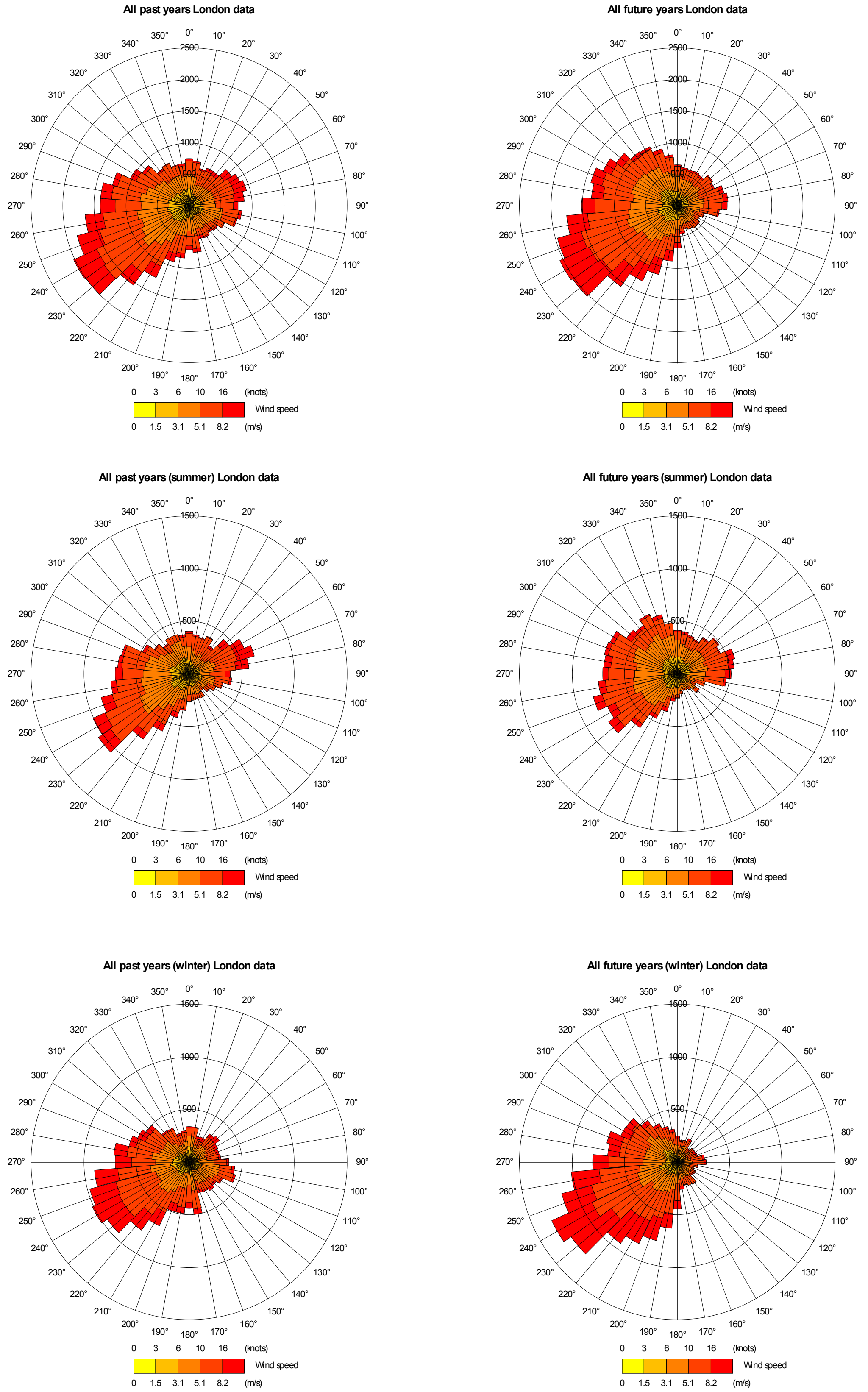

Results for cloud cover, incoming solar radiation and surface heat flux are shown in Figures 6 to 8. The model's treatment of cloud amount is not very realistic, with the model producing very few cloud amounts of 1 to 4 oktas. However the differences between the current and future climates may still give useful information. The main change here is during summer months with the results suggesting that cloud cover will decrease in the future. There are few differences between incoming solar radiation for current and future climates. However, during summer months, the midday incoming solar radiation is slightly greater in a future climate as expected from the cloud cover changes. There is also little change in the surface heat flux apart from a greater frequency of very high heat fluxes in summer and a general increase in midday summer heat fluxes in particular as expected from the cloud cover and incoming solar radiation changes.

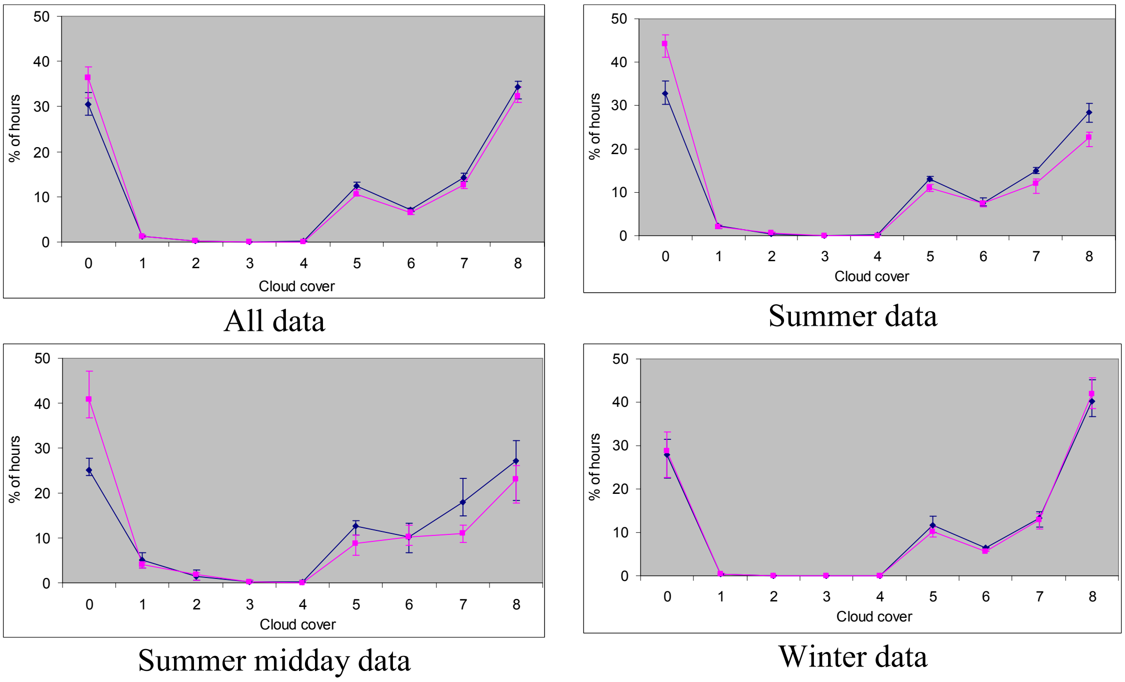

Figure 6: Frequency distribution (%) of cloud cover (oktas) under current and future climate scenarios for London: Current Future

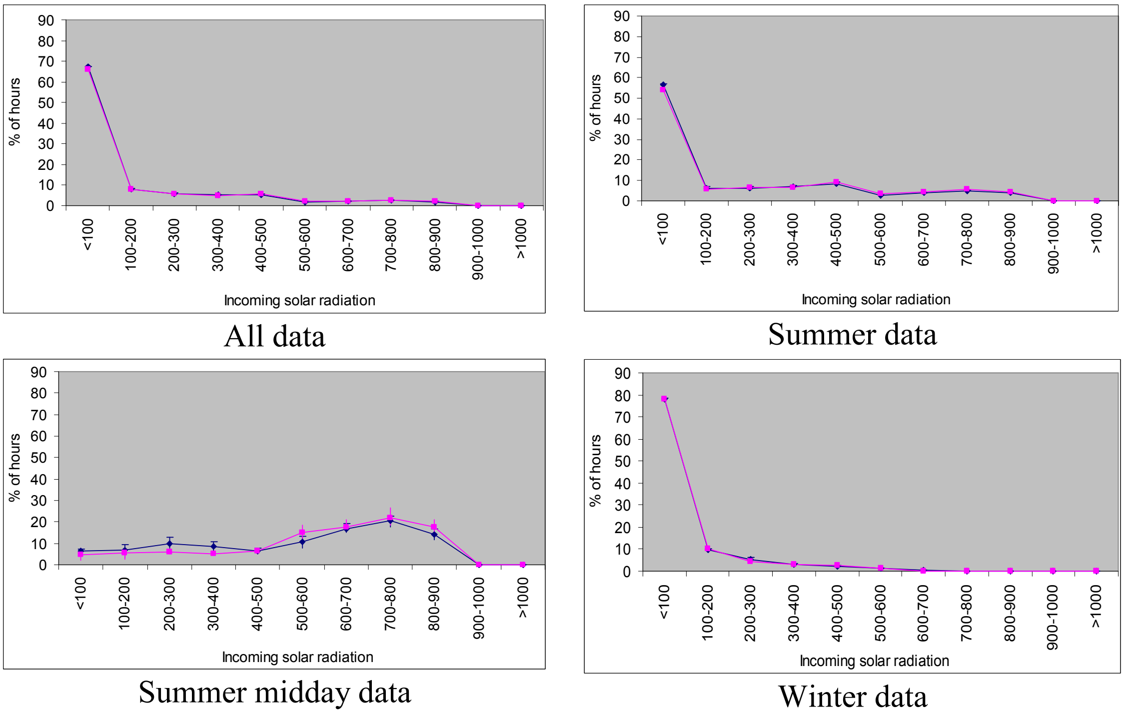

Figure 7: Frequency distribution (%) of incoming solar radiation (W/m^2) under current and future climate scenarios for London: Current Future

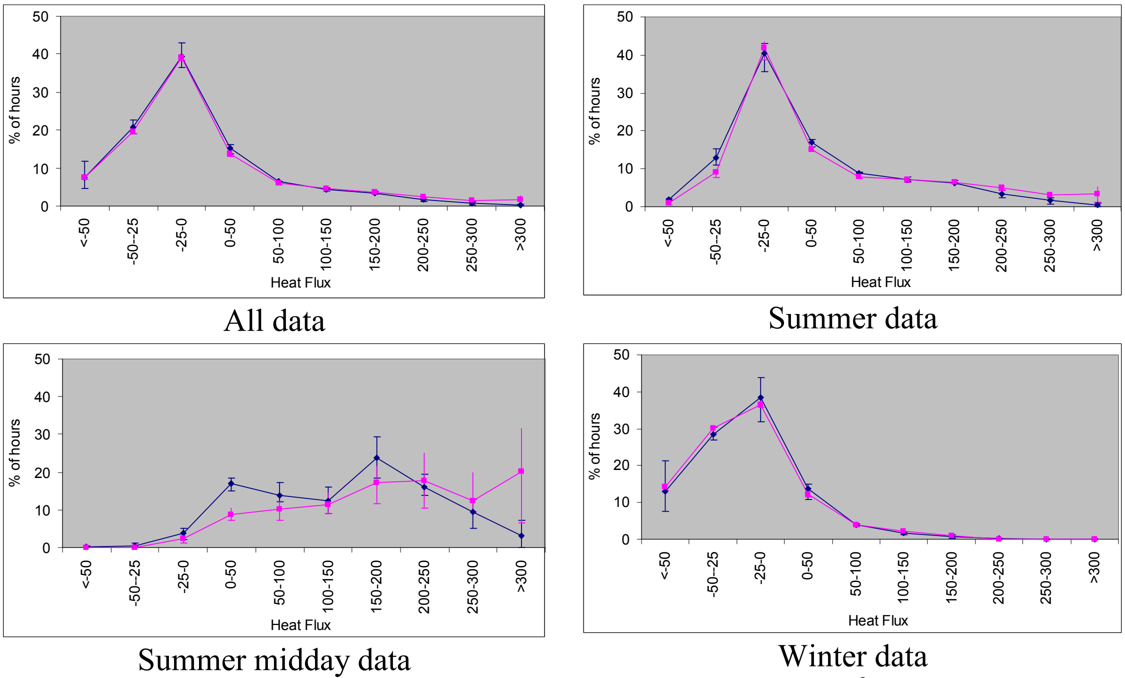

Figure 8: Frequency distribution (%) of surface heat fluxes (W/m^2) under current and future climate scenarios for London: Current Future

Results for boundary layer depth are shown in Figure 9. It is clear from scatter plots (not shown) that the boundary layer depths in the model tend to cluster around values of 50m, 400m, 800m and 1500m (although intermediate values are also apparent). This may be a feature of the model's vertical resolution. This produces somewhat strange looking frequency distributions which are hard to interpret. There seem to be few differences between boundary layer depths for the current and future climates, although the occurrence of boundary layer depths greater than 1500m may occur slightly more in a future climate during summer months. On average there is an increase in boundary layer depth of about 50m (see Table 1 below). This is to be expected given the change in heat fluxes noted above.

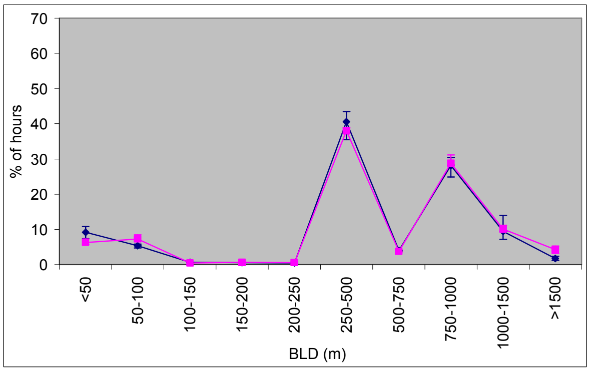

All data

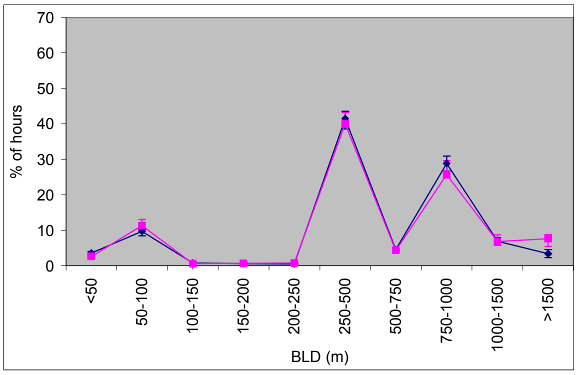

Summer data

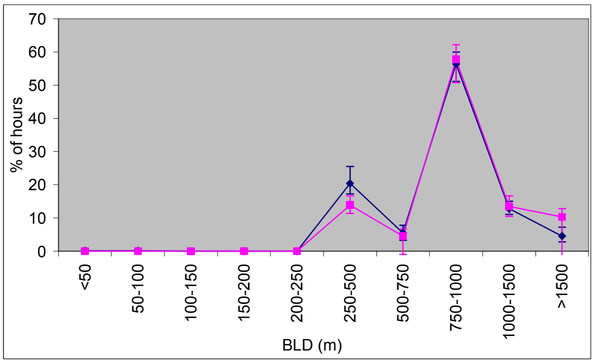

Summer midday data

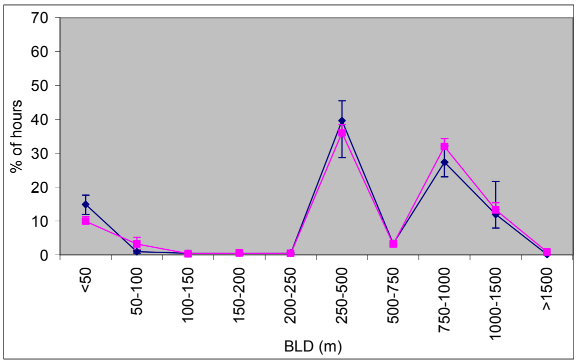

Winter data

Figure 9: Frequency distribution (%) of boundary layer depths (m) under current and future climate scenarios for London: Current Future

Of all the parameters analysed, temperature shows the greatest difference in a future climate compared to the current climate. The results clearly suggest that temperature will be higher in the future in both winter and summer months as expected (see Figure 10). The range of temperatures also seems to increase in summer and reduce in winter. Although we should be cautious in over-interpreting the extremes of the modelled distribution, this suggests that the extremes of summer heat will be greater than expected from the mean warming.

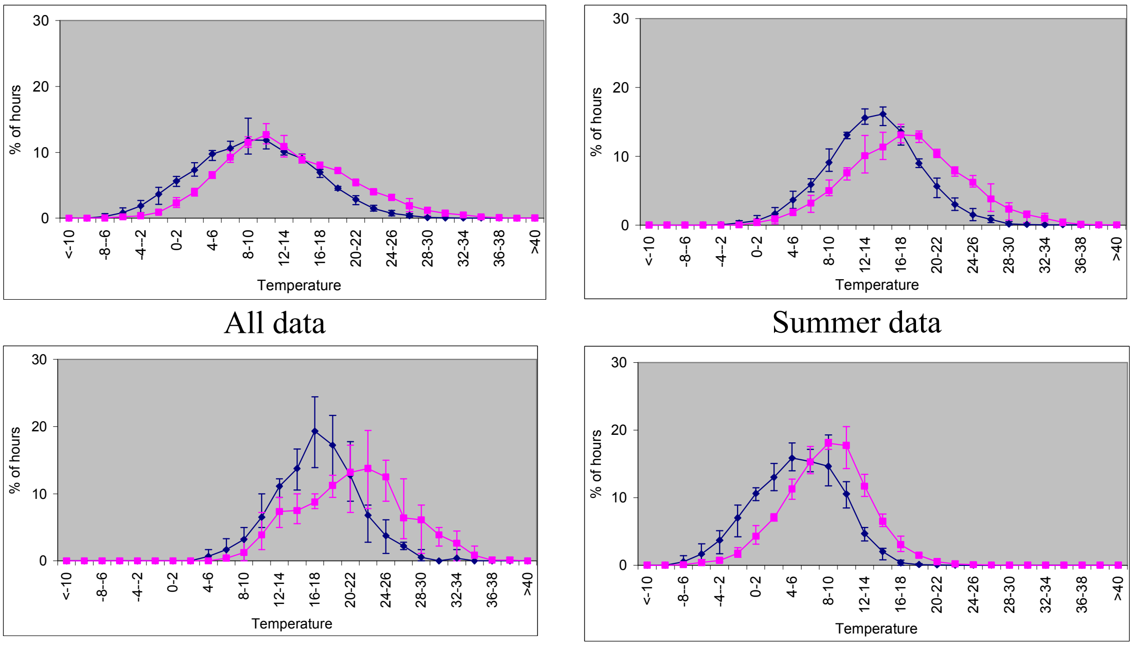

All data

Summer data

Summer midday data

Winter data

Figure 10: Frequency distribution (%) of temperature (^{0}C) under current and future climate scenarios for London: Current Future

The frequency distribution of precipitation is plotted in Figure 11. The lowest range of precipitation, which has a frequency that is off the scale in the graphs, is intended to correspond to dry weather. However there are some complications, which mean this interpretation is not completely straightforward. Firstly the model produces a lot of very small precipitation amounts and so some threshold (0.05 mm/hr is chosen here) needs to be used. Results are not as insensitive to this choice as one would like. Secondly the model precipitation is intended to represent the value over the grid square, and so the occurrence of rain in the model should be interpreted as rain occurring somewhere in the grid square. The model results suggest that during the summer, precipitation will be on average slightly lower in the future, with more periods of no precipitation (Figure 11). In contrast there is a slight increase in precipitation during the winter.

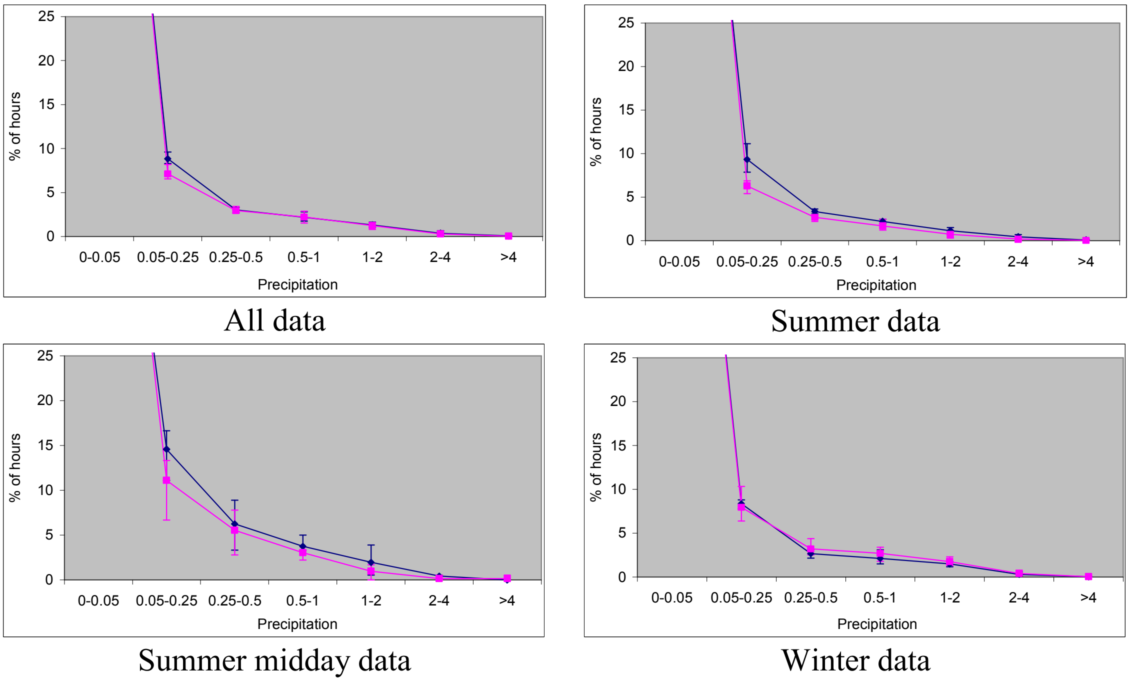

Figure 11: Frequency distribution (%) of precipitation (mm/hr) under current and future climate scenarios for London: —◆— Current —■— Future

Results for mean sea level pressure are shown in Figure 12. The results suggest that during the summer months in the future, the pressure in London will be generally higher. During winter months the opposite is true, with lower pressures more prevalent. This suggests more blocking weather patterns during summer and more mobile westerlies during winter. This has some support from the wind direction analysis above. However these deductions must be tentative, since one cannot unambiguously infer circulation types from pressure at one location.

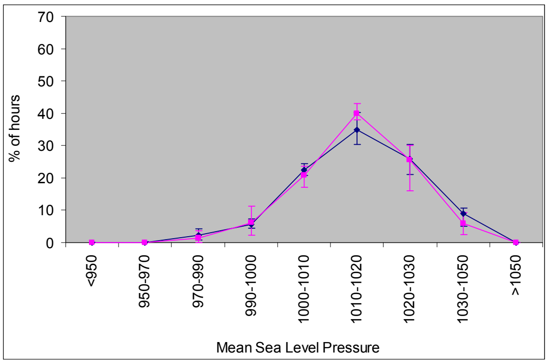

All data

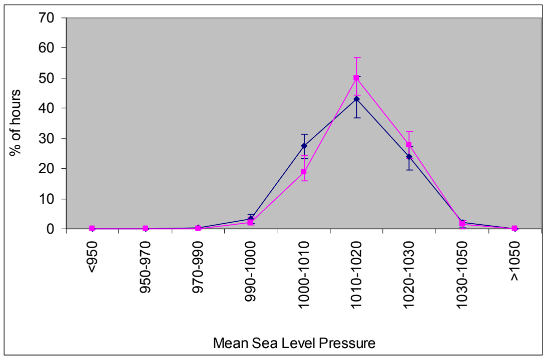

Summer data

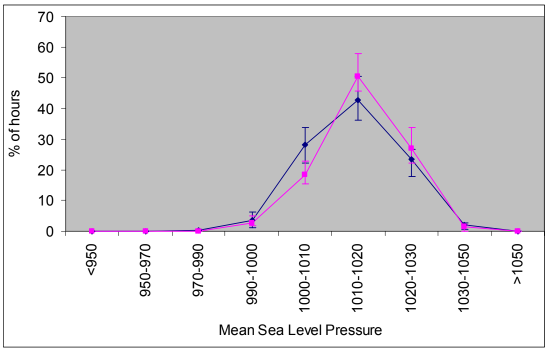

Summer midday data

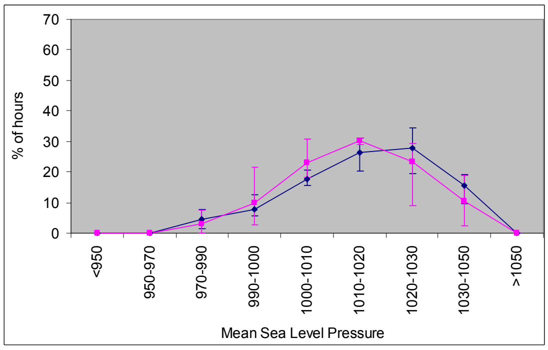

Winter data

Figure 12: Frequency distribution (%) of mean sea level pressure (mb) under current and future climate scenarios for London: Current Future

Results for specific humidity are shown in Figure 13. Specific humidity is slightly higher in the future climate, consistent with the idea that a warmer atmosphere can carry more moisture.

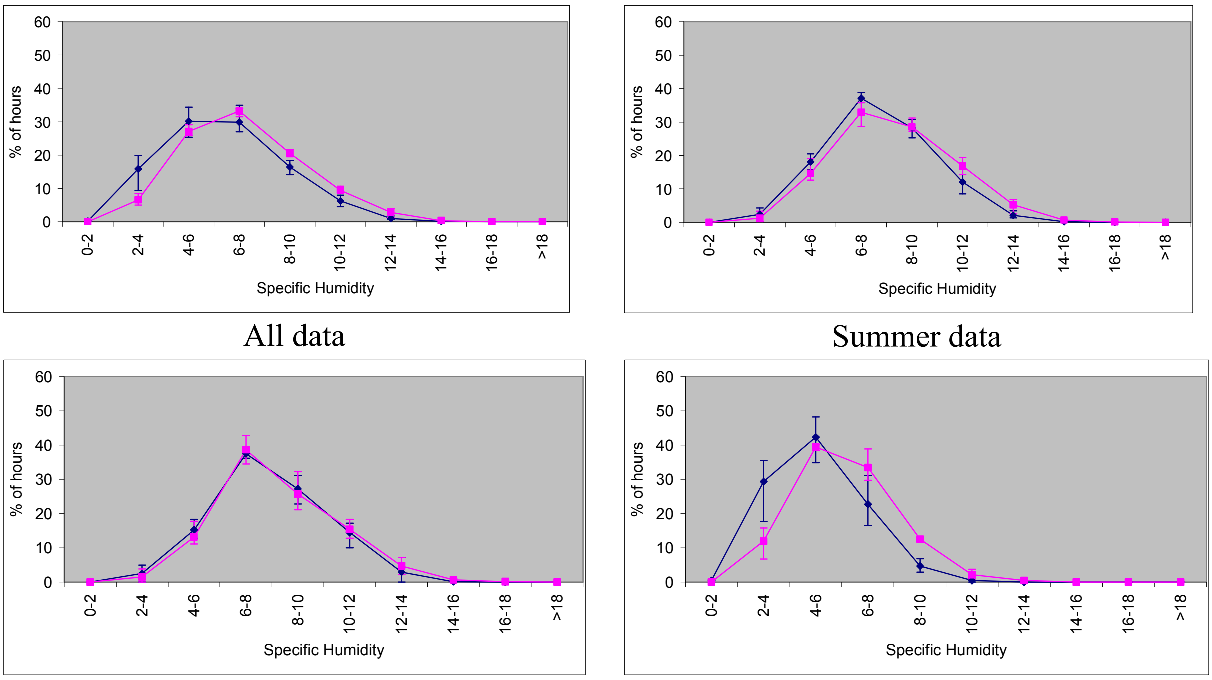

Summer midday data Winter data

Figure 13: Frequency distribution (%) of specific humidity (g/kg) under current and future climate scenarios for London: Current Future

The above analysis shows that, of the variables considered, temperature is the one with the largest signal. The increase in temperature might be expected to lead to increases in isoprene emissions from vegetation, leading to more summer ozone episodes. However, in such episodes the ozone takes time to build up and so the frequency distribution does not provide all the information we need to assess this.

As a result we have looked in more detail at the temperature data to identify the occurrence of prolonged heat wave events, such as the recent August 2003 episode. These events are usually associated with high pressure over the UK, high temperatures and lots of sunshine – the ideal conditions for the production of ozone. Generally, the longer the conditions persist, the greater the ozone concentrations produced.

We define a heat wave event as a period when the maximum temperature on consecutive days exceeds 25ºC. The summer (April to September) data was analysed to determine the number and duration of heat wave events for each year. The results for 1971, 1976, 1981 and 1986 were averaged to produce values for the "current climate" and the results for 2071, 2076, 2081 and 2086 were averaged to produce values for the "future climate".

The results are shown in Figure 14. The graph clearly shows that a future climate has more periods of days with maximum temperatures above 25°C, and that these periods last for a longer time. For example, for the current climate data, the maximum number of consecutive days when the daily maximum temperature is greater than 25°C is 8, yet for the future climate data it is 22.

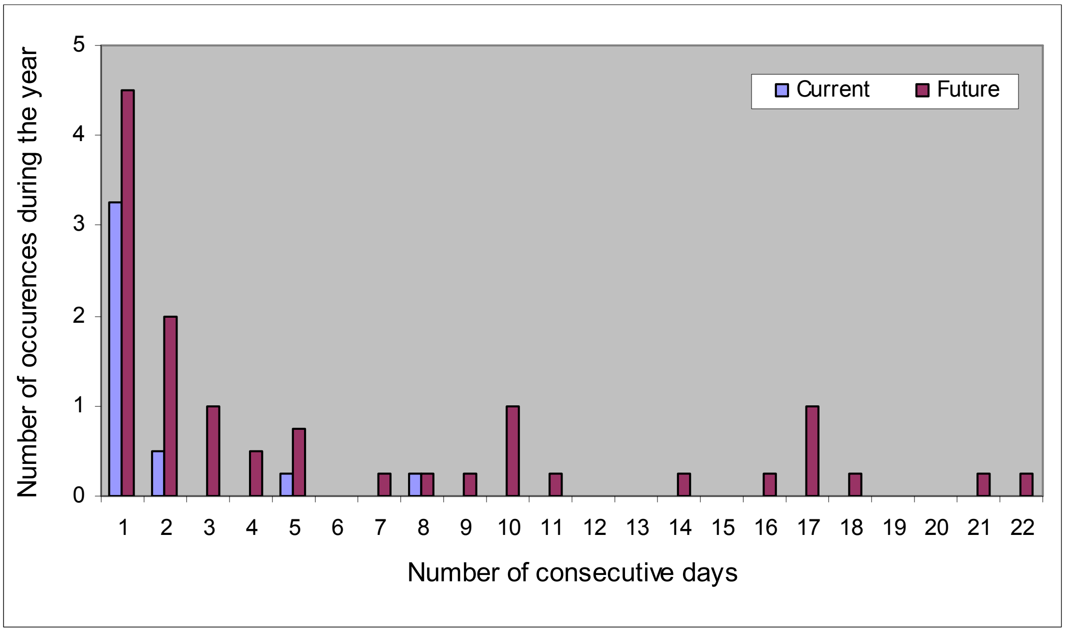

Figure 14: Average number of heat wave events of given duration per year, a heat wave event being a period where the maximum temperature each day is above 25 °C. Values are given for the modelled current climate and future climate for London.

Table 1 gives an overall summary of the meteorological data for London. This shows annual averages and ranges for each of the meteorological variables for each of the years. Overall results are also presented which combine all four 'current' years and combine all four 'future' years. Table 1 paints a picture consistent with the graphs and wind roses and shows that the most significant impacts are on temperature with limited changes in the other variables.

As well as the variables discussed above, the surface latent heat flux has been included in Table 1. The mean latent heat flux is smaller in the future climate for London, which is consistent with the expectation of dryer soils (see Hulme et al., 2002). This probably also contributes to the increase in surface sensible heat flux.

Table 1. Met data summary – London

		1971	1976	1981	1986	1971-86	2071	2076	2081	2086	2071-86
Wind speed (m/s)	Min	0.0	0.1	0.1	0.1	0.0	0.2	0.1	0.1	0.1	0.1
	Max	15.4	15.8	16.9	17.1	17.1	18.7	15.9	15.5	16.2	18.7
	Mean	5.0	4.9	5.6	4.9	5.1	5.0	5.3	5.2	5.1	5.2
Mean wind vector	Speed (m/s)	0.6	1.1	2.2	1.3	1.3	1.7	1.9	1.7	2.4	1.9
	Direction (^{0})	242	245	252	249	249	254	245	264	264	257
Cloud cover (oktas)	Min	0	0	0	0	0	0	0	0	0	0
	Max	8	8	8	8	8	8	8	8	8	8
	Mean	4.8	5.2	5.0	5.1	5.0	4.6	4.9	4.4	4.5	4.6
Incoming solar radiation (W/m^2)	Min	0	0	0	0	0	0	0	0	0	0
	Max	865	851	858	868	868	855	842	854	856	856
	Mean	139	134	135	134	136	146	143	149	144	145
Surface heat flux (w/m^2)	Min	-97	-94	-103	-111	-111	-110	-104	-98	-85	-110
	Max	375	372	293	347	375	429	394	426	431	431
	Mean	13	11	3	10	9	19	17	23	15	18
Boundary layer depth (m)	Min	47.2	47.4	47.3	47.3	47.2	47.6	47.4	47.5	47.8	47.4
	Max	1587	1532	1558	1543	1587	1600	1590	1590	1578	1600
	Mean	565	559	642	538	576	613	631	570	615	621
Temperature (^{0}C)	Min	-7.3	-6.3	-6.3	-7.6	-7.6	-5.2	-6.5	-6.7	-3.1	-6.7
	Max	36.5	27.9	28.6	29.0	36.5	37.6	41.3	37.1	32.7	41.3
	Mean	9.6	10.1	10.0	9.3	9.8	13.6	13.2	13.2	12.8	13.2
Precipitation (mm/hr)	Min	0.0	0.0	0.0	0.0	0.0	0.0	0.0	0.0	0.0	0.0
	Max	5.2	10.4	5.2	5.2	10.4	6.0	5.8	6.6	3.4	6.6
	Mean	0.06	0.07	0.09	0.07	0.07	0.06	0.08	0.05	0.07	0.07
	Total	512mm	579mm	748mm	606mm	4×611mm	503mm	730mm	423mm	566mm	4×555mm
Mean sea level pressure (mb)	Min	975.0	980.2	968.9	961.6	961.6	968.6	972.2	980.9	990.8	968.6
	Max	1040.0	1039.4	1041.8	1045.1	1045.1	1036.6	1041.4	1043.1	1040.9	1043.1
	Mean	1015.9	1016.4	1013.0	1015.4	1015.2	1015.5	1011.4	1017.1	1016.0	1015.0
Specific humidity (kg/kg)	Min	0.0016	0.0021	0.0018	0.0018	0.0016	0.0023	0.0022	0.0021	0.0024	0.0021
	Max	0.0161	0.0138	0.0163	0.0152	0.0163	0.0156	0.0161	0.0176	0.0156	0.0176
	Mean	0.0062	0.0065	0.0065	0.0064	0.0064	0.0072	0.0074	0.0070	0.0072	0.0072
Surface latent heat flux (W/m^2)	Min	-28	-31	-26.5	-44	-44	-25	-27	-22	-22	-27
	Max	467	422	559	496	559	378	431	438	417	438
	Mean	38	40	47	41	42	34	38	33	40	36

2.2(ii) Results for Glasgow

In Figures 15 to 27 and Table 2 we present the analysis of the Glasgow meteorological data from the climate model simulations. For wind (Figures 15 and 16) the results are similar to London, although the summer wind speed differences are much smaller and the summer wind direction changes are now more similar to those in winter, with an increase in westerlies and a reduction in easterlies in the modelled future climate. As for London results are broadly consistent with those in Hulme et al. (2002) although, as noted above, Hulme at al. point out that wind changes tend to differ between different climate simulations and so should not be regarded as very reliable.

Wind roses for each of the years analysed are shown in Figure 17 while Figure 18 shows a wind rose combining all four past years, a wind rose combining all four future years, plus wind roses of summer and winter conditions. Figure 17 shows an increase in the duration of winds from the WSW and reduction in the duration of winds from the ENE by something of the order of 200 hours per 10 degree sector. This change is rather more marked than that seen for London and it seems rather consistent between the different years, i.e. the change is greater than the year to year variability. This change is also clear in the top row of Figure 18 which shows the combined results from all years. Splitting the results into winter and summer cases, further insight is gained (Figure 18). During the current climate, the winds during the winter months, although predominately WSW, still show some preference for other directions. In the future climate, the winds are focusing towards a more predominant WSW direction with a large increase in the number of cases from that direction. During the summer months in the current climate, an almost equal preference between WSW and ENE winds occurs. This is not the case in the future climate (right) where the shift to almost entirely WSW winds is clearly evident.

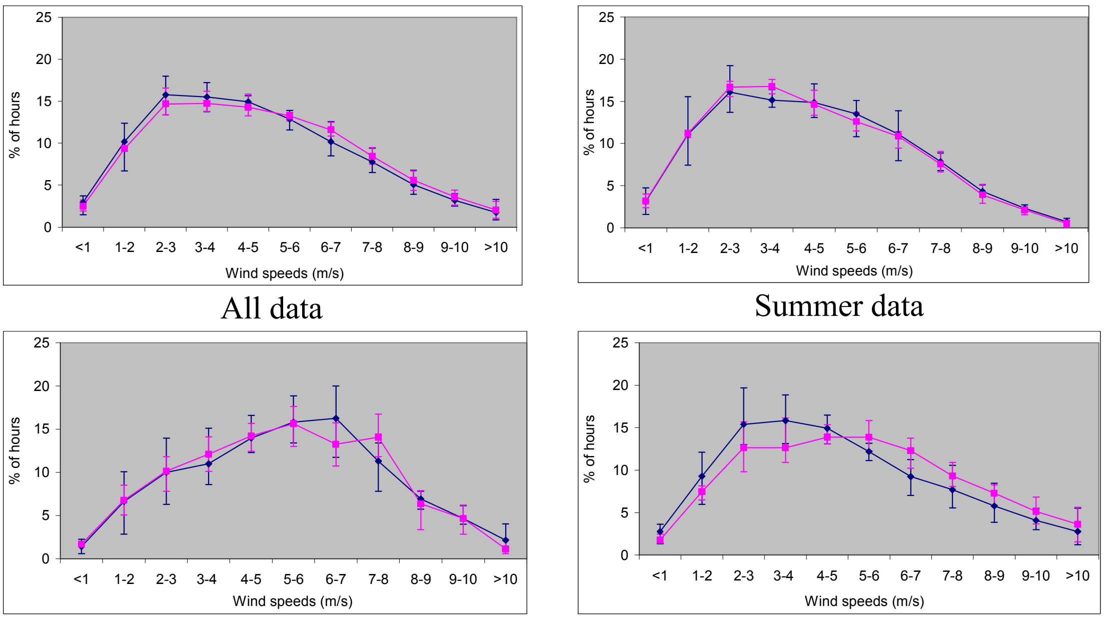

Figure 15: Frequency distribution (%) of wind speeds (m/s) under current and future climate scenarios for Glasgow: —◆— Current —■— Future

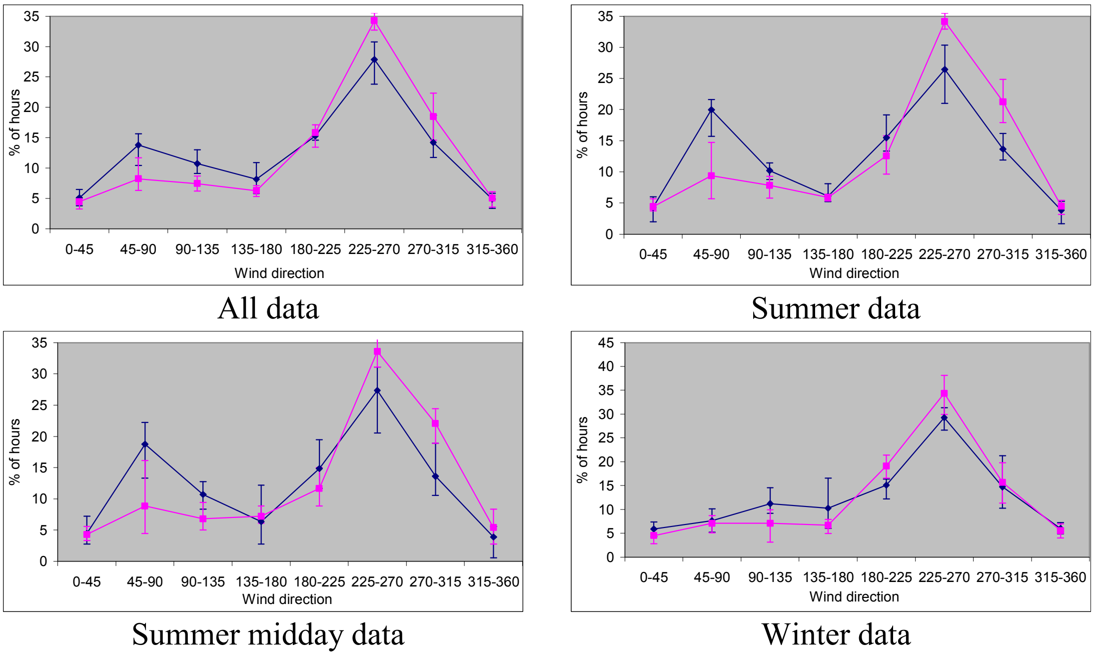

Figure 16: Frequency distribution (%) of wind direction (^{0}) under current and future climate scenarios for Glasgow: Current Future

Figure 17: Wind roses for Glasgow under the current and future climate scenarios, given separately for each of the years considered.

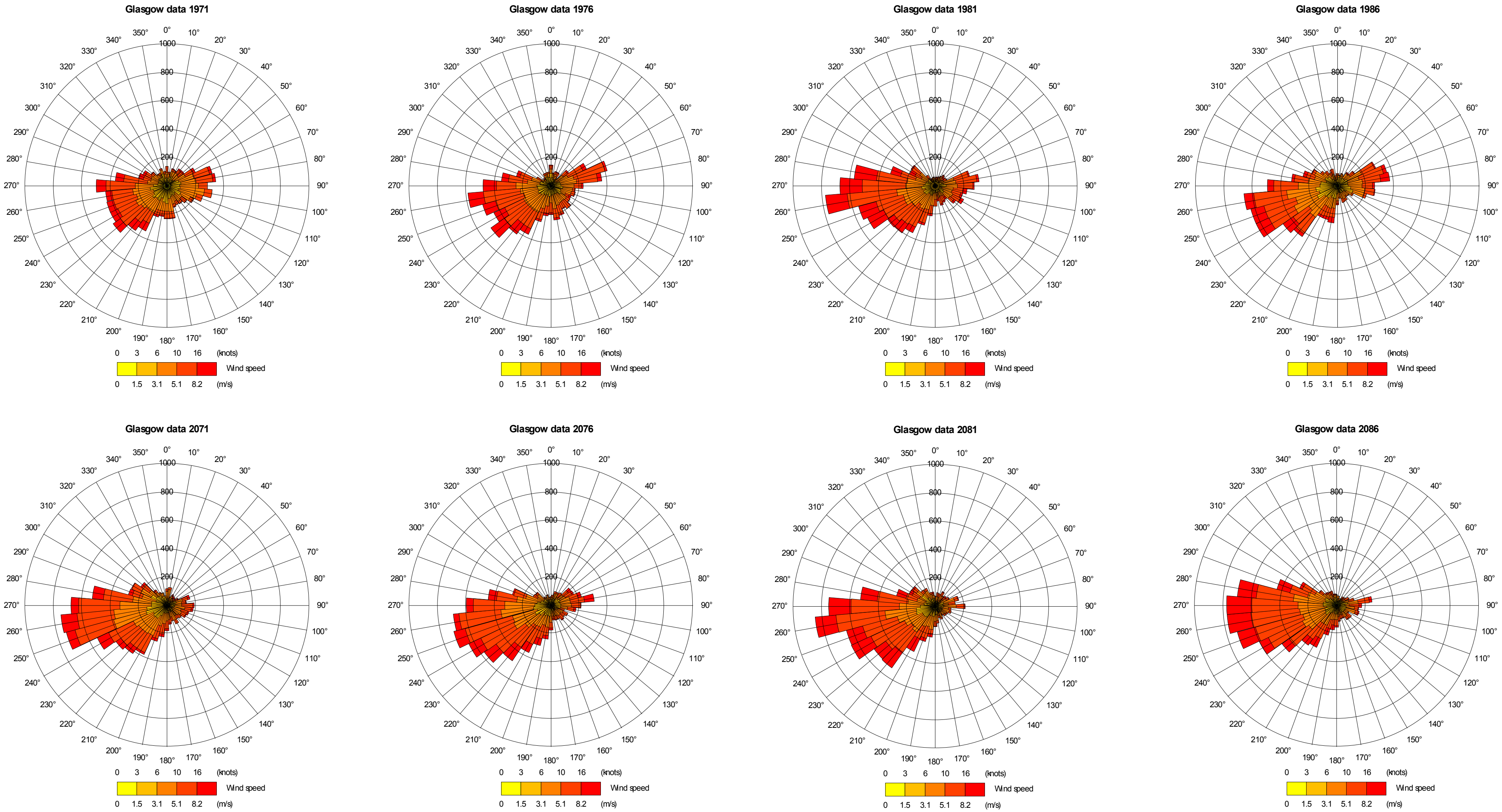

Figure 18: Wind roses for Glasgow under the current and future climate scenarios. All year, summer, and winter roses are presented. For each scenario, the results are for the four years combined.

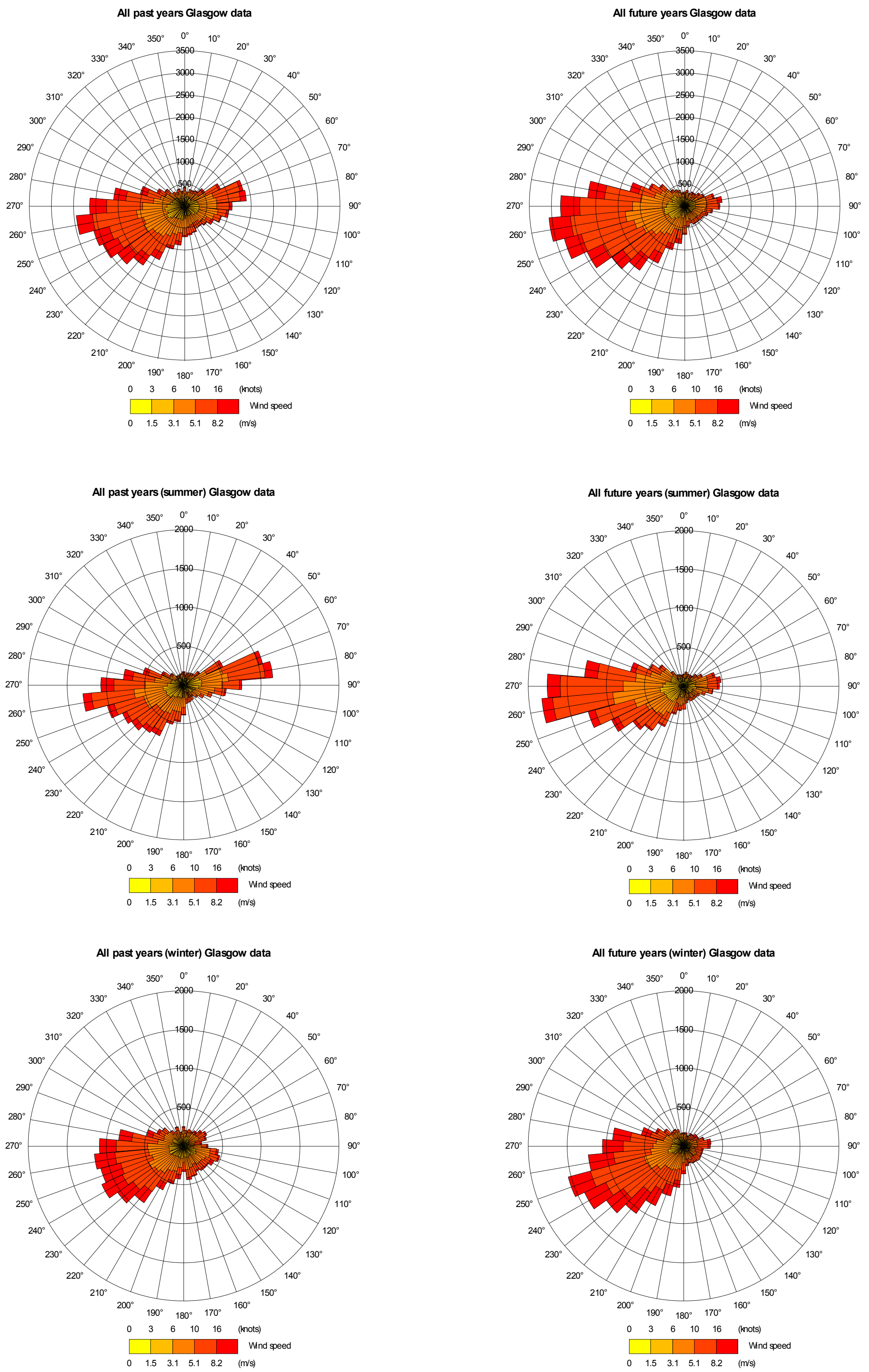

Results for cloud cover, incoming solar radiation and surface heat flux are given in Figures 19 to 21. The changes are qualitatively very similar to those for London although are somewhat smaller for radiation and heat flux. No significant changes in the distribution of boundary layer depth (Figure 22) are observed for Glasgow although there is a small increase in the mean depth of ~10m (see Table 2 below).

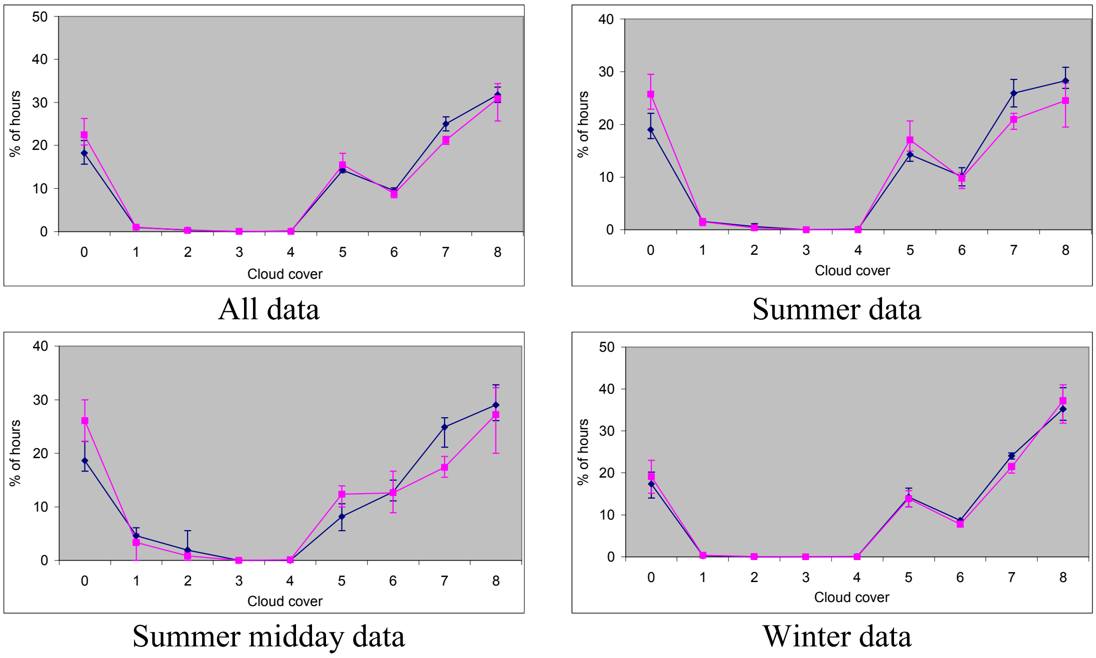

Figure 19: Frequency distribution (%) of cloud cover (oktas) under current and future climate scenarios for Glasgow: Current Future

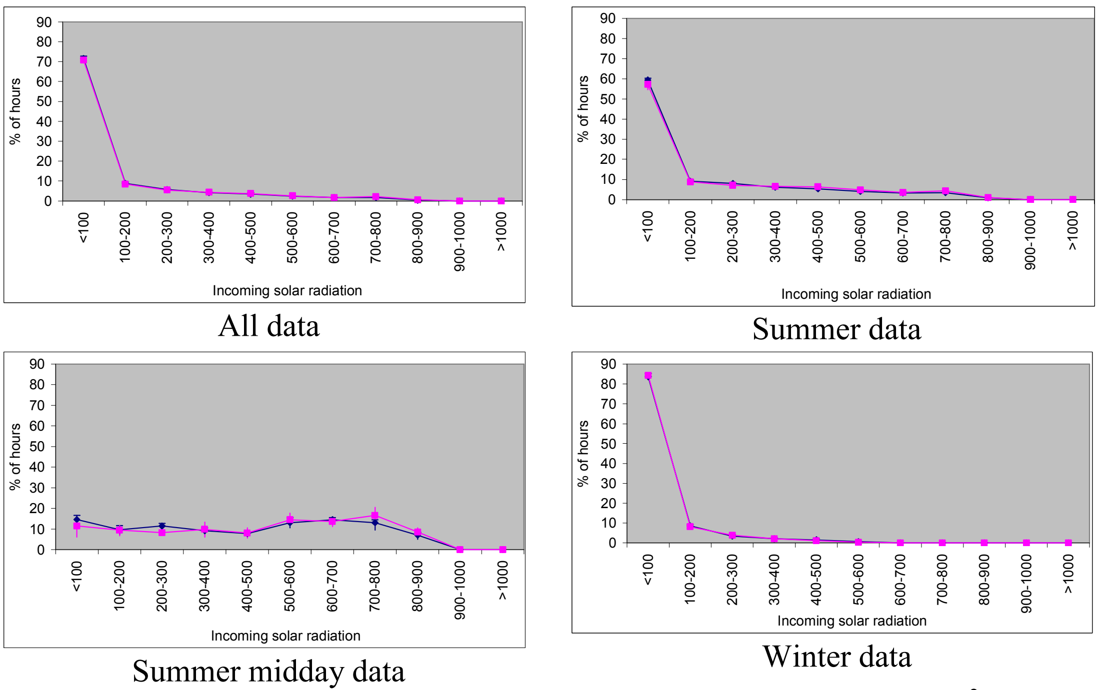

Figure 20: Frequency distribution (%) of incoming solar radiation (W/m^2) under current and future climate scenarios for Glasgow: Current Future

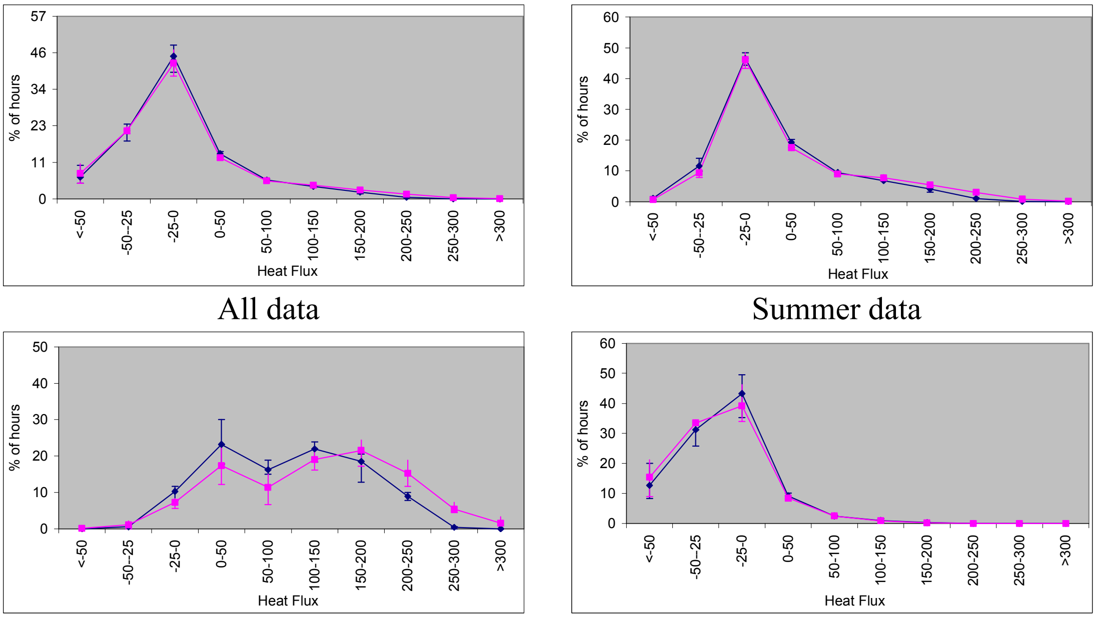

All data | Summer data

Summer midday data | Winter data

Figure 21: Frequency distribution (%) of surface heat fluxes (W/m^2) under current and future climate scenarios for Glasgow: Current Future

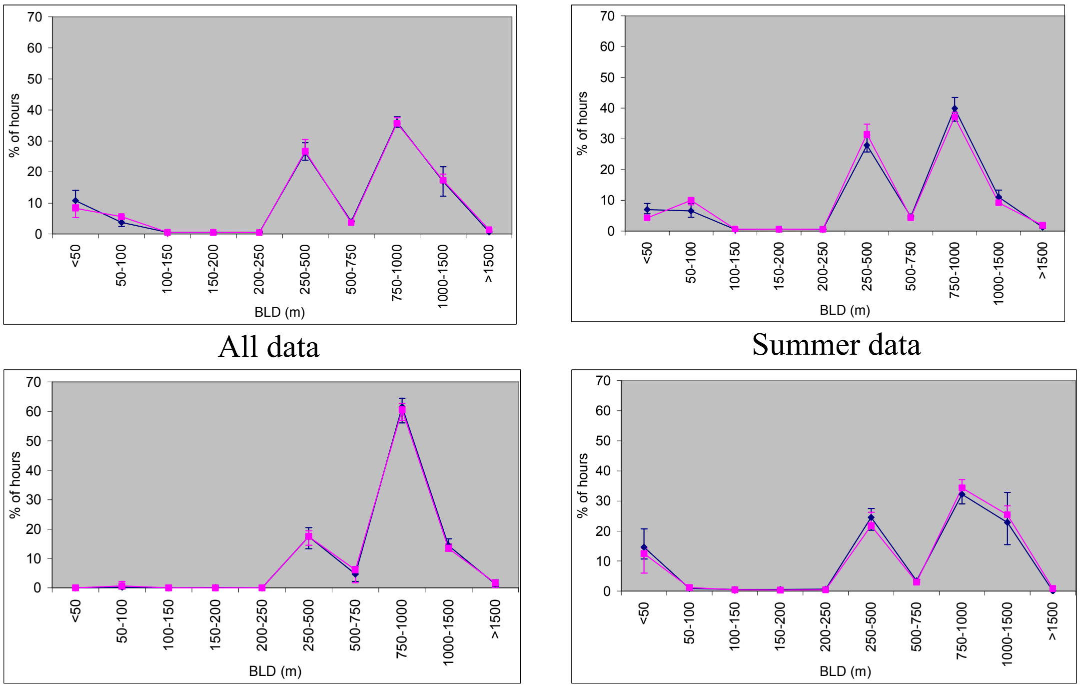

All data | Summer data

Summer midday data | Winter data

Figure 22: Frequency distribution (%) of boundary layer depths (m) under current and future climate scenarios for Glasgow: Current Future

As for London, there is a very clear difference for temperature (Figure 23), with significant increases throughout the year. The increased range of temperatures seen for London is not apparent here however and, if anything, there is a slight reduction in the winter range. The precipitation (Figure 24) shows a decrease in summer and an increase in winter as for London, although the changes are a little larger than those for London.

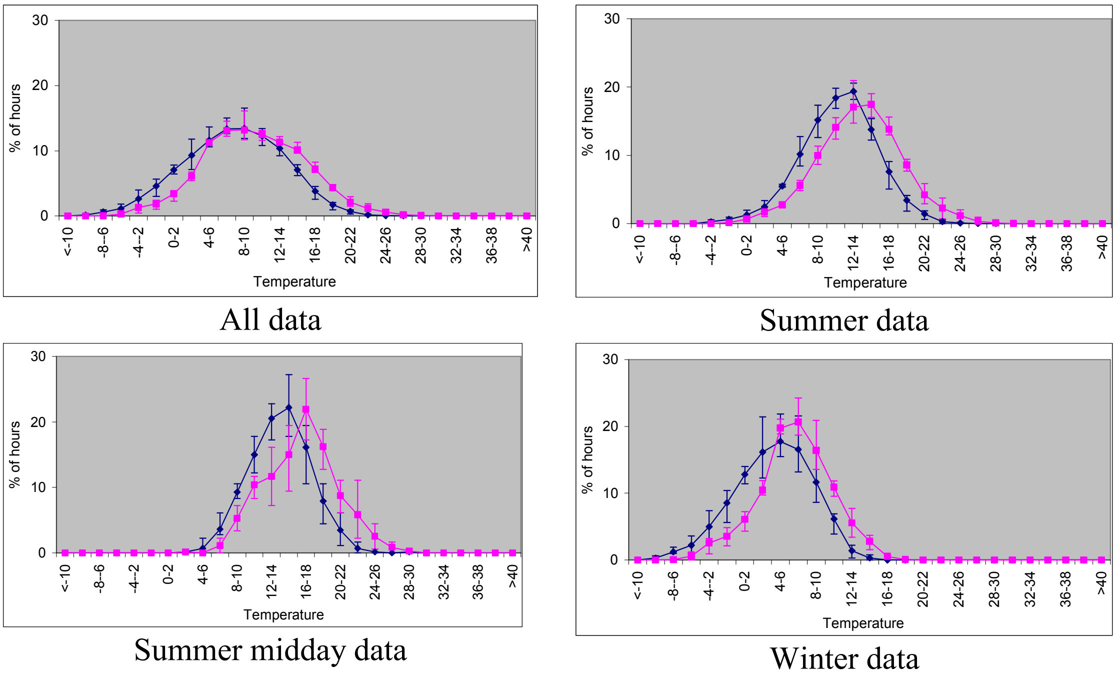

Figure 23: Frequency distribution (%) of temperature (^{0}C) under current and future climate scenarios for Glasgow: Current Future

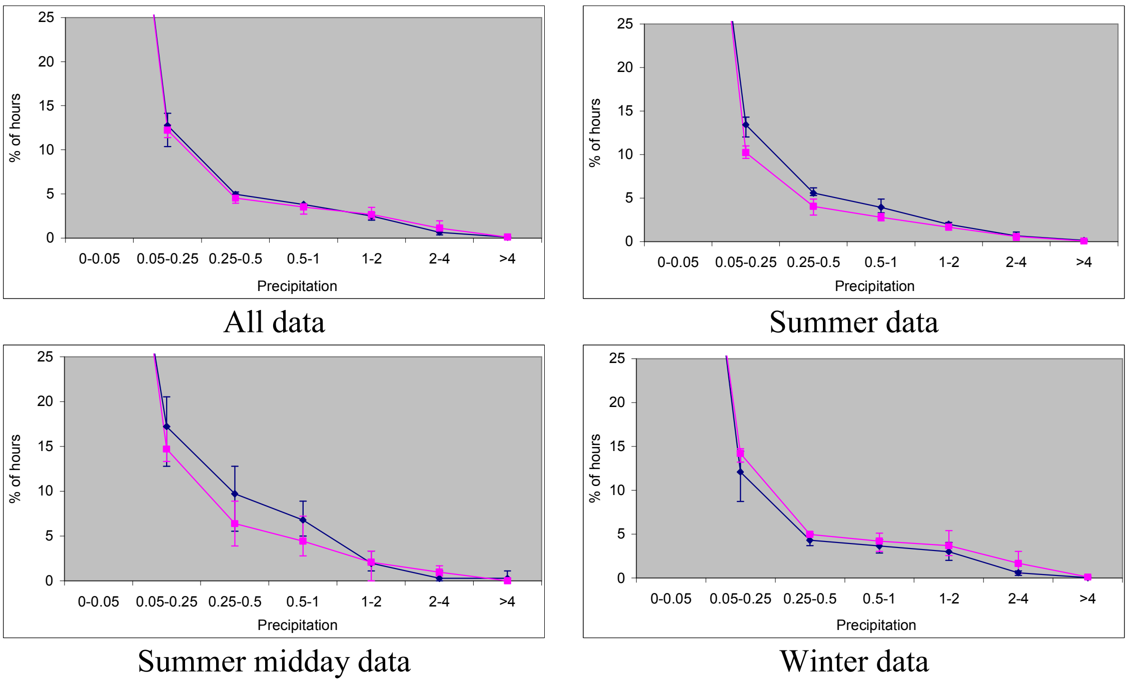

Figure 24: Frequency distribution (%) of precipitation (mm/hr) under current and future climate scenarios for Glasgow: Current Future

Figure 25 shows that the mean sea level pressure shows very similar behaviour to London with a tendency to higher pressures in summer and lower in winter. As before this suggests an increase in blocking patterns in summer and in mobile weather systems in winter.

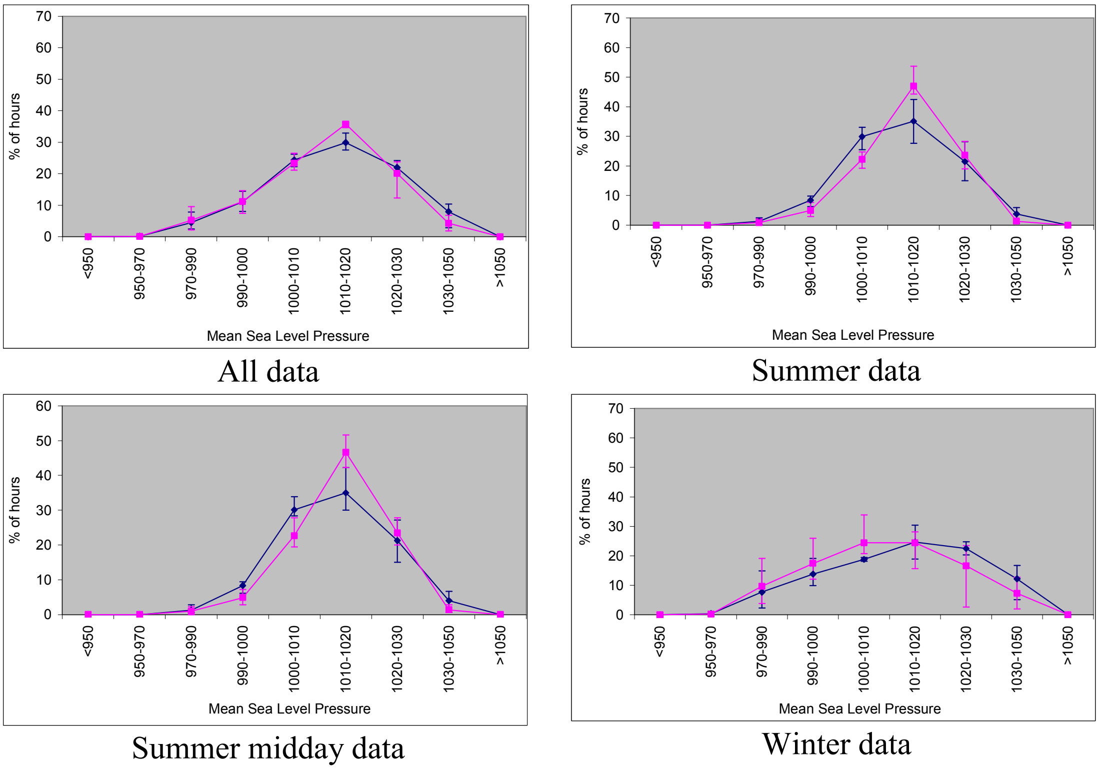

Figure 25: Frequency distribution (%) of mean sea level pressure (mb) under current and future climate scenarios for Glasgow: Current Future

Results for specific humidity are shown in Figure 26. As for London, the specific humidity is slightly higher in the future climate, consistent with the idea that a warmer atmosphere can carry more moisture.

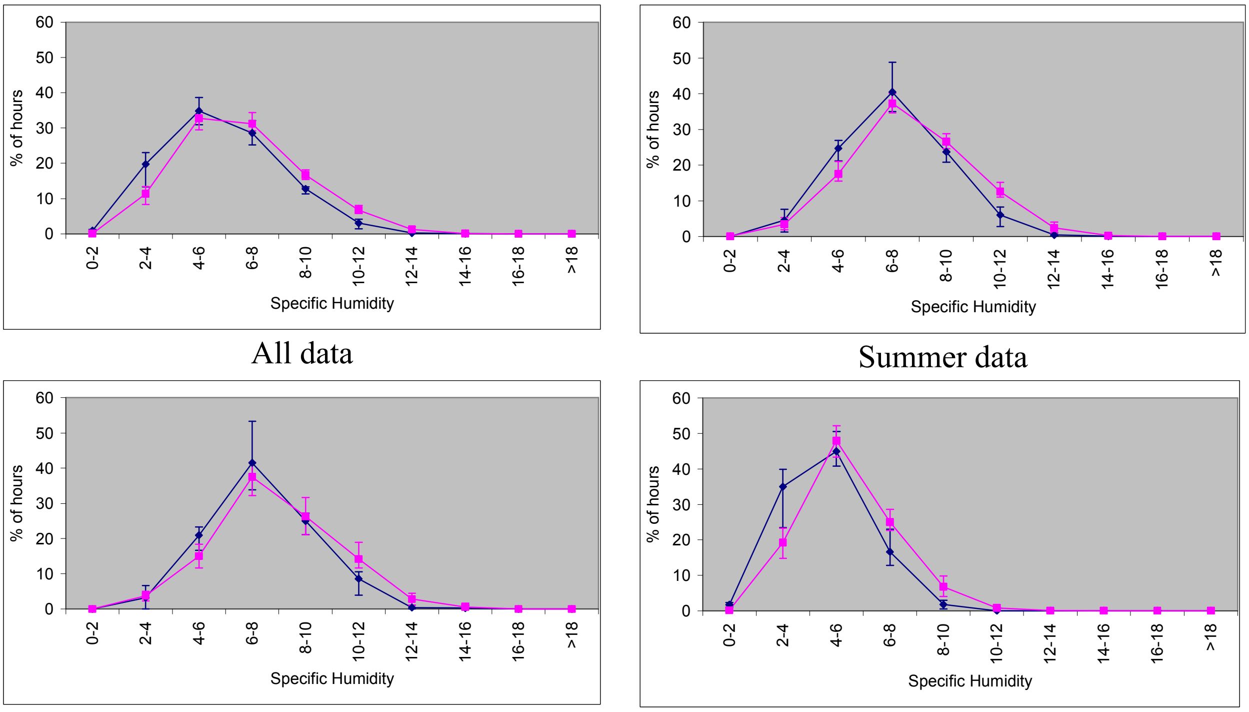

All data

Summer data

Summer midday data

Winter data

Figure 26: Frequency distribution (%) of specific humidity (g/kg) under current and future climate scenarios for Glasgow: Current Future

The occurrence of heat wave events was investigated as for London. The number of heat wave events is much smaller for Glasgow than for London (see Figure 27) as expected given the cooler climate. However a substantial increase in frequency is predicted.

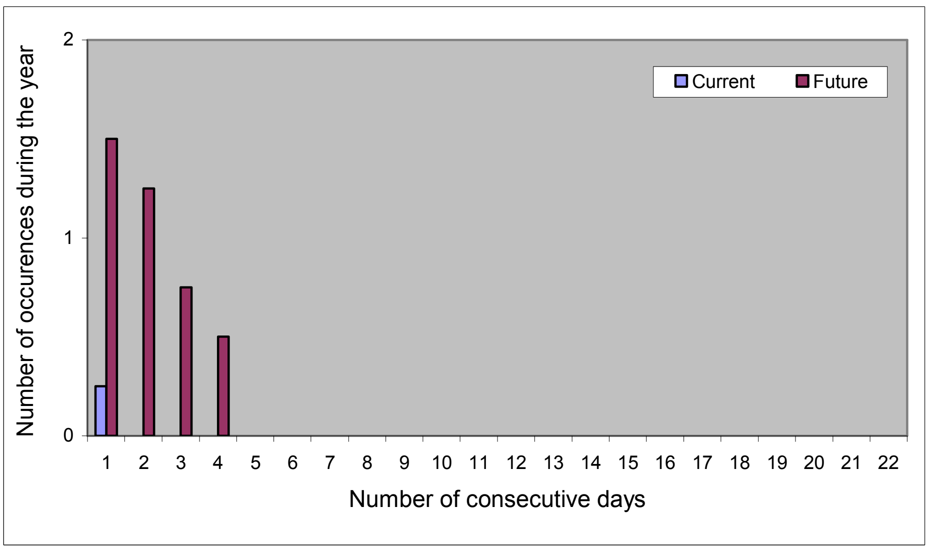

Figure 27: Average number of heat wave events of given duration per year, a heat wave event being a period where the maximum temperature each day is above 25 °C. Values are given for the modelled current climate and future climate for Glasgow.

Table 2 gives an overall summary of the meteorological data for Glasgow. Table 2 shows that, as for London, the most significant impacts are on temperature with limited changes in the other variables.

As well as the variables discussed above, the surface latent heat flux has been included in Table 2. The substantial decrease in surface latent heat flux predicted for London is not repeated for Glasgow. This is consistent with the expectation that the tendency towards dryer soils is much greater in the south of the country (Hulme et al., 2002).

Table 2. Met data summary – Glasgow

		1971	1976	1981	1986	1971-86	2071	2076	2081	2086	2071-86
Wind speed (m/s)	Min	0.0	0.0	0.1	0.1	0.0	0.1	0.0	0.1	0.0	0.0
	Max	13.6	12.9	15.2	14.2	15.2	16.6	16.4	15.5	14.3	16.6
	Mean	4.4	4.8	5.4	4.5	4.8	4.7	4.9	5.1	5.1	4.9
Mean wind vector	Speed (m/s)	1.2	1.6	2.3	1.4	1.6	2.3	2.3	3.0	3.0	2.6
	Direction (^{0})	229	225	242	238	235	245	235	250	251	246
Cloud cover (oktas)	Min	0	0	0	0	0	0	0	0	0	0
	Max	8	8	8	8	8	8	8	8	8	8
	Mean	5.9	6.1	5.7	5.9	5.9	5.6	5.7	5.2	5.7	5.5
Incoming solar radiation (W/m^2)	Min	0	0	0	0	0	0	0	0	0	0
	Max	837	835	834	835	837	830	825	833	837	837
	Mean	111	103	111	104	107	113	112	121	109	114
Surface heat flux (w/m^2)	Min	-90	-127	-105	-113	-127	-109	-104	-99	-98	-109
	Max	251	260	268	259	268	328	278	329	362	362
	Mean	1	-1	-2	1.5	0	5	4	5	2	4
Boundary layer depth (m)	Min	47.2	47.0	47.2	46.9	46.9	47.6	47.3	47.7	47.7	47.3
	Max	1539	1524	1529	1544	1544	1538	1548	1554	1531	1554
	Mean	658	696	747	607	677	655	683	701	726	691
Temperature (^{0}C)	Min	-7.9	-10.1	-8.5	-9.2	-10.1	-7.1	-6.2	-4.7	-3.9	-7.1
	Max	29.7	21.5	23.0	25.7	29.7	30.3	26.0	29.8	25.4	30.3
	Mean	7.9	8.4	7.8	7.1	7.8	10.1	10.0	10.3	10.2	10.1
Precipitation (mm/hr)	Min	0.0	0.0	0.0	0.0	0.0	0.0	0.0	0.0	0.0	0.0
	Max	8.1	4.5	6.1	5.9	8.1	5.6	5.9	5.6	4.3	5.9
	Mean	0.13	0.12	0.13	0.11	0.12	0.11	0.17	0.11	0.13	0.13
	Total	1098mm	1003mm	1082mm	920mm	4×1026mm	970mm	1458mm	962mm	1139mm	4×1132mm
Mean sea level pressure (mb)	Min	965.4	976.6	958.9	963.2	958.9	975.2	959.3	978.9	978.5	959.3
	Max	1039.8	1042.0	1037.6	1044.0	1044.0	1038.5	1040.9	1043.1	1045.0	1045.0
	Mean	1014.0	1013.9	1009.2	1013.1	1012.5	1012.6	1007.8	1013.7	1012.0	1011.5
Specific humidity (kg/kg)	Min	0.0015	0.0011	0.0015	0.0016	0.0011	0.0014	0.0019	0.0018	0.0022	0.0014
	Max	0.0152	0.0124	0.0126	0.0138	0.0152	0.0164	0.0156	0.0142	0.0133	0.0164
	Mean	0.0059	0.0060	0.0058	0.0057	0.0059	0.0067	0.0066	0.0064	0.0066	0.0066
Surface latent heat flux (W/m^2)	Min	-35	-63	-61	-45	-63	-70	-27	-20	-27	-70
	Max	402	432	361	416	432	364	367	418	367	418
	Mean	39	39	42	35	39	38	37	39	38	38

2.2(iii) Summary of meteorological changes

The most obvious impact of climate change is on temperature with limited changes in other parameters. Increases of order 2-4 ^{0}C are predicted with larger increases in London than Glasgow. Also, in the London summer, the width of the distribution increases, suggesting that the extremes of summer heat increase by more than this. Other changes with potential impacts on air quality are as follows:

- **Wind speed:** Increases in winter and reductions in summer are predicted at both locations. The main effect is likely to be a change in pollutant dilution at its source, although there will also be some changes through the consequent changes in stability.
- **Wind direction:** In London there is a tendency for more westerlies in winter and a shift from south-westerlies to north-westerlies in summer. In Glasgow there is a tendency for wind directions to become much more concentrated in the WSW direction. For Glasgow this is likely to lead to the impacts from large point sources being more concentrated in one sector, and hence higher. More generally the wind direction will influence the extent to which polluted air from Europe or cleaner air from the Atlantic is present.
- **Cloud cover:** This shows a small reduction in summer at both sites, and a modest consequential increase in incoming solar radiation (increasing photochemical production of ozone) and surface heat flux (increasing the ability of the boundary layer to disperse pollutants, but bringing pollutants from elevated sources to the ground more rapidly). There is little change in winter.
- **Boundary layer depth:** This is influenced by wind speed, surface heat flux and lapse rate above the boundary layer and shows a modest mean increase in London (~50m) and a very small mean increase in Glasgow (~10m). Increasing boundary layer depth has a similar effect to increased surface heat flux, increasing the dispersive ability of the boundary layer.
- **Precipitation:** This decreases in summer and increases in winter at both sites, and is relevant to air quality because of the ability of precipitation to wash out pollutants.
- **Mean sea level pressure:** This is not directly relevant to air quality, but is related to the type of circulation pattern and so has some relation with the other variables considered here and with factors not addressed by these variables such as the degree of boundary layer venting by convective clouds. It is predicted to become higher in summer and lower in winter, suggesting an increase in blocking circulation patterns in summer and in mobile westerly patterns in winter.
- **Specific humidity:** This is predicted to increase at both sites. It plays a significant role in ozone chemistry, generally enhancing its destruction.

3. Impact of climate change upon air dispersion

Possible impacts of climate change on air quality are many. They include changes in dispersion and chemical transformations over a wide range of scales, changes in source characteristics brought about by changes in energy use and 'technological' developments, and changes in the size and nature of natural sources, for example the likely increase in biogenic emissions with temperature. In this study the emphasis is on the changes in dispersion and chemical transformation that will occur with the emphasis on the local to regional scale. However the study also touches on changes in emissions, both through the empirical 'rural predictor' model (see Section 3.2) which will implicitly take some account of changes in biogenic emissions with temperature, and through the STOCHEM model simulations (see Section 3.3) which allow for changes in anthropogenic (but not biogenic) emissions.

Three types of calculation are presented. Firstly the impact of the changes in the characteristics of the atmospheric boundary layer on dispersion of primary pollutants from single sources is considered using the dispersion model ADMS 3.2 (CERC, 2001) and the air quality model ADMS-Urban (McHugh et al, 1997). Secondly the impacts on urban air quality are estimated using (i) the air quality model ADMS-Urban (McHugh et al, 1997) to calculate the impacts on dispersion and chemical transformation across the urban area, and (ii) a statistical 'rural predictor' model to estimate impacts on background concentrations advected into the urban areas. In the study concentrations of NO_x, NO_2, PM_{10} and O_3 are calculated. Finally production of 'regional' ozone at London and Glasgow as calculated by the STOCHEM models are presented.

3.1 Dispersion of primary pollutants from single sources

The first set of dispersion calculations was used to assess the impact of changing meteorology directly on the dispersion of primary pollutants as might, for example, arise from changes in the wind speed and direction and the boundary layer stability and depth (§2.2). Dispersion calculations were carried out for the primary pollutant NO_x for the following four sources:

- A small non-buoyant point source
- A large point source (small power station stack)
- A large power station
- A straight long road

These dispersion calculations were conducted using ADMS 3.2 (CERC, 2001) for the point sources and ADMS-Urban (McHugh et al, 1997) for the road source. The sources have each been modelled using the four years of past meteorological data (1971, 1976, 1981 and 1986) and the four years of future predicted meteorology (2071, 2076, 2081 and 2086) for London and for Glasgow. Modelling was carried out using hourly sequential air temperature, wind speed, wind direction, precipitation and cloud cover data, as given in Section 2.

The calculations were made over a 6 km × 6 km grid with 50 × 50 points (16 km ×16 km with 31 × 31 points for the large power station) with the emission source centered in the middle; in each case the surface roughness was taken as 0.5m, a typical urban value. The road source was 10m wide and 6km long running East-West across the output area centered on y=0. The emission rate along the road was 1 g km^{-1} s^{-1} of NO_x. Other modelling parameters are shown in Table 3.

Table 3. Point source details

	Small point source	Small power station	Large power station
Height (m)	20	93	259
Diameter (m)	0.5	2.7	19
Exit velocity (m/s)	0	22	23
Temperature (^oC)	Ambient	168	91
NO_x emission rate (g/s)	1	9.15	1568

3.1(i) Results for London

The calculated annual average ground level NO_x results from the London meteorological data are shown in Figure 28 for each of the four sources and for current years and future years. Table 4 shows the spatial maximum over the whole output grid of various NO_x concentration statistics. The statistics considered are the annual average, the maximum hourly average, and the 99.8th, 99th and 98th percentiles of the hourly average.

The table and graphs show that the impact of climate change on both the pattern of concentration and maximum concentrations is relatively limited for the London meteorological dataset with greatest impacts generally being less than 10% for both annual and short term averages. An exception is the case of the large power station which, as perhaps might be expected, exhibits larger increases in annual-average and 98th-percentile concentrations. These increases are likely to be due both to the tendency to a greater preponderance of westerlies which will concentrate the impact more into one sector, and to increases in surface heat flux and boundary layer height which will allow more pollutant to be brought down to the ground as a result of the deeper boundary layer and more vigorous convective turbulence. (We should point out that the surface heat flux and boundary layer depth used to obtain these modelled results is not that presented in Section 2 but is that estimated within ADMS from cloud cover etc. However, we expect deeper day-time boundary layers with larger heat fluxes to be produced in ADMS, driven by the cloud and wind speed changes shown in Figures 2 and 6 and in Table 1.) Conversely the concentration decreases for the road source, probably also due to an increase in convective turbulence. The small power station and small point source show intermediate behavior, at least in terms of the annual average and lower percentiles (the high percentiles are likely to be much more strongly affected by inter-annual variability especially for our relatively small samples of just 4 years), with generally only limited impact of the changes in the meteorological datasets.

To put the changes in context it is useful to consider the results of Davies and Thomson (1997). They considered two sources roughly equivalent to the small point source and large power station in Table 4, looked at variability of results over a number of one year, three year and five year periods, and compared the results with those for a ten year period. Substantial variability was observed from year to year, but the (spatial peak of the) 3 and 5 year averages and 98th-percentiles all agreed with the longer term 10 year results to within 9%. Based on this we tentatively conclude that the increases in the annual average and 98th-percentiles for the large power station source are likely to be statistically significant, but the other changes may not be.

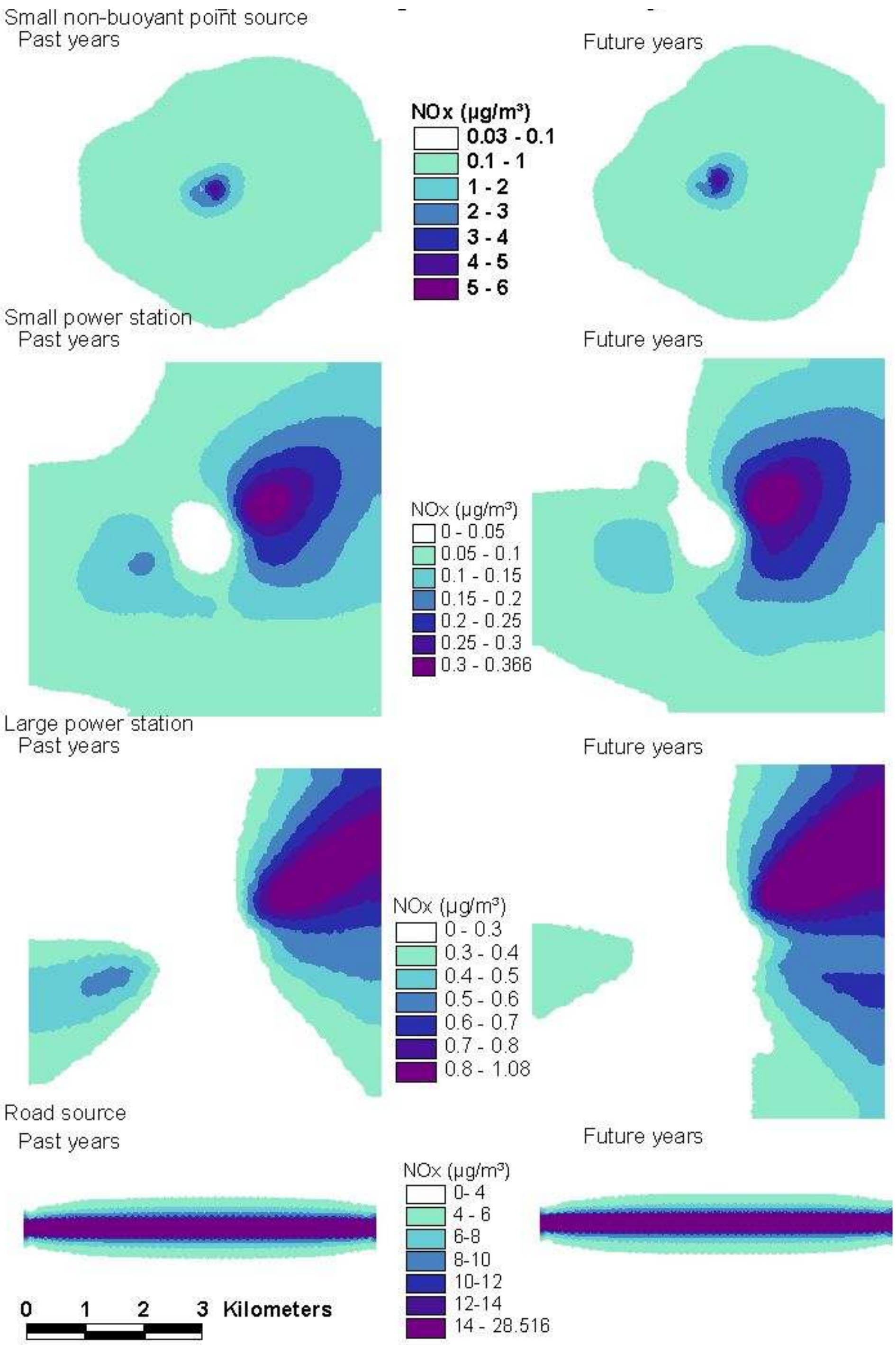

Figure 28: Long term average of NO_x for past (1971, 1976, 1981, 1986) and future years (2071, 2076, 2081, 2086) calculated using ADMS 3.2 (point sources) and ADMS-Urban (road source) with London meteorological data. Note the scale bar does not relate to the large power station plot which covers 16×16km; all other plots are 6×6km and do relate to the scale bar.

Table 4. Calculated spatial maxima of various NO_x concentration statistics: London meteorological data

		Annual average (µg/m³)	Maximum hourly average (µg/m³)	99.8th percentile of hourly average (µg/m³)	99th percentile of hourly average (µg/m³)	98th percentile of hourly average (µg/m³)
Small point	Past	5.54	342.6	130.3	57.31	46.19
	Future	5.58	365.4	120.7	55.45	45.77
	% change	0.7	6.7	-7.4	-3.2	-0.9
Small power station	Past	0.347	10.48	6.59	4.80	4.25
	Future	0.366	10.98	6.59	4.97	4.28
	% change	5.5	4.8	0.0	3.5	0.7
Large power station	Past	0.95	94.12	50.69	31.77	18.85
	Future	1.07	97.39	47.04	33.65	21.26
	% change	12.63	3.47	-7.20	5.92	12.79
Road	Past	28.52	866.85	655.13	464.64	347.49
	Future	27.46	858.11	659.46	439.05	335.60
	% change	-3.7	-1.0	0.7	-5.5	-3.4

3.1(ii) Results for Glasgow

The annual average NO_x results are shown in Figure 29. Table 5 shows the spatial maximum over the whole output grid of various NO_x concentrations statistics, namely the annual average together with various percentiles of hourly averages.

Table 5 shows a predicted increase due to climate change of over 25% in the spatial maximum of the NO_x annual average concentrations for the three modelled point sources. The contour plots, Figure 29, are consistent with this being mainly associated with the marked increase, much greater than in the case of London, in the predominance of westerly winds (see the wind roses in Figures 17 and 18 and, for comparison, the London wind roses in Figures 4 and 5). The greater predominance of westerly winds will tend to concentrate the impact into one sector, leading to greater values for the spatial peaks of the concentration statistics. The reduced cloud cover, leading to increased heat fluxes and greater convection, may also be a factor. However, it would be expected that this would also affect the peak concentrations (maximum hourly average, 99.8th percentile) and these show little change, except for the maximum concentration resulting from the small point source which decreases.

Referring again to the results of Davies and Thomson (1997) we judge that the increases in the (spatial peak of the) annual average results for the point sources and in the 98th and 99th percentiles for the large power station source are almost certainly statistically significant. The other changes in Table 5 may not be. We include here the 16% decrease in the maximum hourly average for the small point source. Although this seems a large change, the overall maximum is always likely to show more statistical scatter than other results. Also the change could be affected by a small move in the location of the maximum, the limited resolution of the output grid, and the fact that the peak occurs very close to the source for this source.

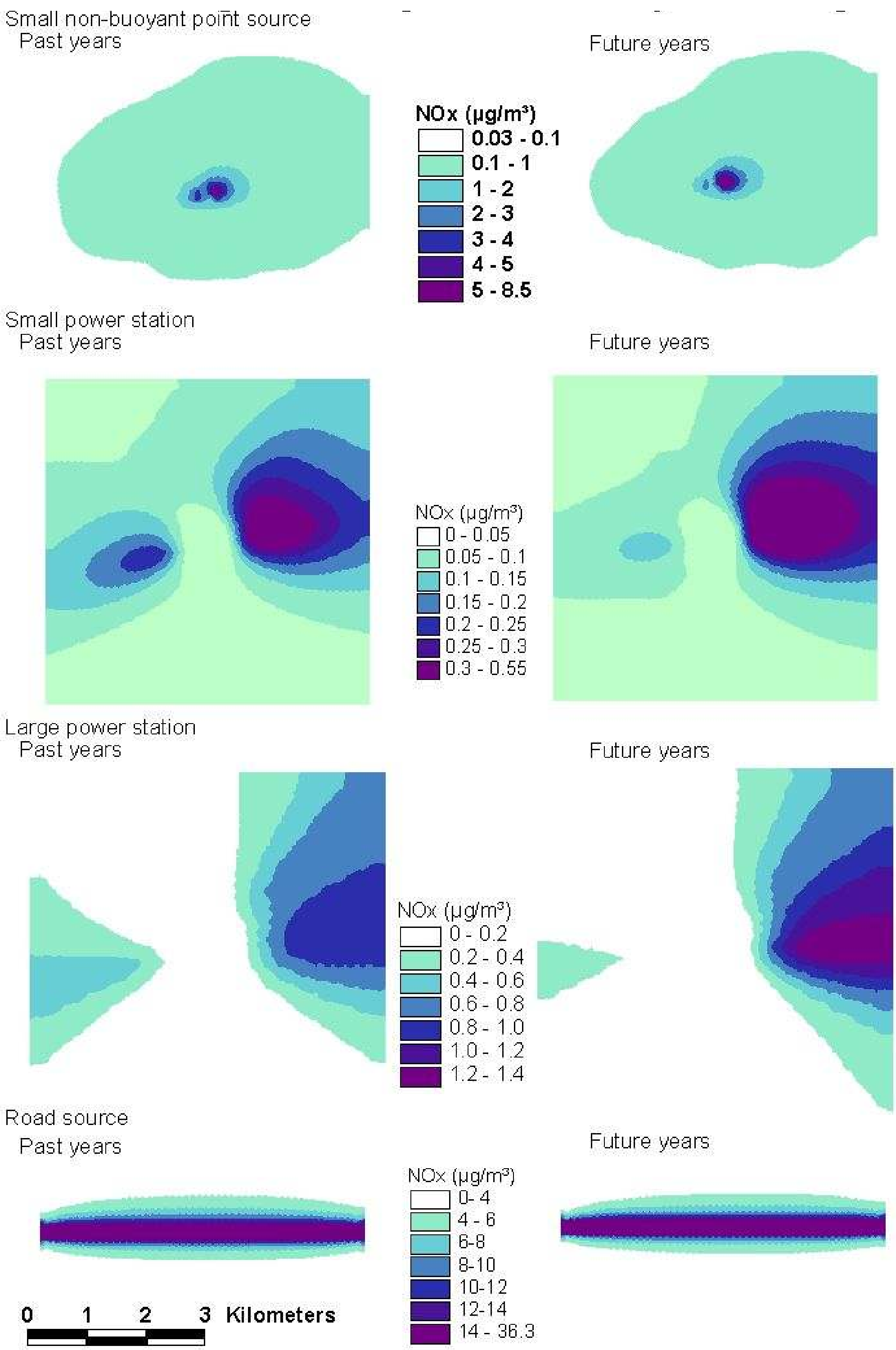

Figure 29: Long term average of NO_x for past (1971, 1976, 1981, 1986) and future years (2071, 2076, 2081, 2086) calculated using ADMS 3.2 (point sources) and ADMS-Urban (road source) with Glasgow meteorological data. Note the scale bar does not relate to the large power station plot which covers 16×16km; all other plots are 6×6km and do relate to the scale bar.

Table 5. Calculated spatial maxima of various NO_x concentration statistics: Glasgow meteorological data

		Annual average (µg/m³)	Maximum hourly average (µg/m³)	99.8th percentile of hourly average (µg/m³)	99th percentile of hourly average (µg/m³)	98th percentile of hourly average (µg/m³)
Small point	Past	6.82	405.83	141.92	59.89	49.91
	Future	8.53	341.66	144.82	62.22	52.20
	% change	25.07	-15.81	2.04	3.89	4.59
Small power station	Past	0.41	12.81	6.66	5.22	4.44
	Future	0.55	12.35	6.81	5.59	4.78
	% change	34.15	-3.59	2.25	7.09	7.66
Large power station	Past	0.98	89.40	47.19	30.71	18.71
	Future	1.36	88.53	49.71	36.07	25.92
	% change	38.78	-0.97	5.34	17.45	38.54
Road	Past	36.34	883.19	702.99	491.45	393.97
	Future	33.65	868.49	668.37	470.18	363.13
	% change	-7.40	-1.66	-4.92	-4.33	-7.83

3.2 Impacts on Urban Pollution

In Section 3.1 some modelling calculations of the dispersion of primary pollutants from typical point and road sources have shown that the impact of climate change on the concentration of primary pollutants arising from single sources is likely to be relatively modest for the case of London but more significant for Glasgow. In this section we consider the impacts of climate change on overall air quality within two urban areas (London and Glasgow) and estimate both local dispersion effects and also regional/local ozone impacts and the generation of nitrogen dioxide.

No direct account is taken of changes in emissions in future years, arising either from business as usual scenarios or as a consequence of climate change effects. At first sight this implies that the calculations illustrate merely the direct impacts of local/regional changes in meteorology, assuming that no other impacts are taking place. However some indirect impacts of changes in biogenic emissions may be included through the use of the empirical 'rural predictor' model (see below).

The dispersion modelling has been conducted using ADMS-Urban and emissions inventories for the local emissions in London and Glasgow. The London inventory is for 2001 and is described by Mattai (2003) while the Glasgow inventory is for 2002 and uses NAEI gridded data (see http://www.naei.org.uk/data_warehouse.php) and Glasgow City Council road and point source data. The modelling was carried out using air temperature, wind speed, wind direction, precipitation and cloud cover data, as given in Section 2. Background concentrations are estimated using CERC's statistically based 'rural predictor' model derived from monitored background concentrations and observed meteorological parameters. The derived functions express concentrations of background pollutant concentration in terms of temperature and wind direction for O_3 and PM_{10}, and in terms of wind speed and wind direction for NO_x and NO_2. Different curves are used in different parts of the UK. The example curve (Figure 30) shows the strong increase of regional O_3 with temperature for temperatures greater than 15ºC. Other trends are less clear; however wind directions associated with air masses from mainland Europe generally have higher pollutant levels. Note that here, and throughout this report, ppb means ppb by volume.

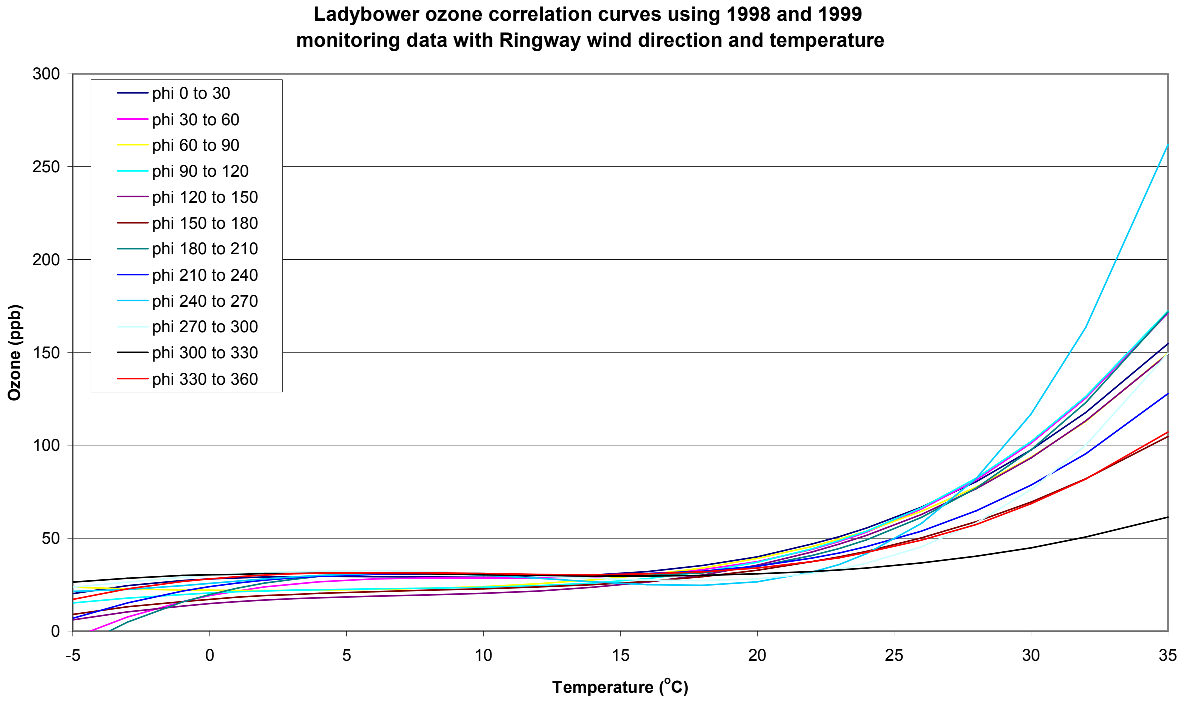

Figure 30: Correlation curves for background pollution – Ozone.

In the rural predictor there are no direct allowances for the effect of changes in emissions or changes in water vapour concentration. The latter is known to impact on ozone concentration at larger scales. However there will be some indirect allowance for changes in emissions (especially biogenic emissions) and water vapour concentration to the extent that these changes are represented by the empirical curves and changes in the input variables temperature, wind speed and wind direction used in the curves.

For future projections it is assumed that the curves retain their current form. While this is a plausible simplifying assumption to make, there are some reasons why it may not be an accurate one and this is a significant source of uncertainty. For example if the dependence of ozone on temperature is due mainly to changes in biogenic emissions of hydrocarbons with temperature, then the curves are likely to remain valid in a changed climate. However the dependence on temperature may be partly due, for example, to dependence on insolation (which drives the photochemistry) which, being higher on clear sky summer days, is correlated with temperature. If this is so, the change in temperature with climate is unlikely to correspond to an equivalent increase in insolation, and hence the empirical curves may misrepresent ozone amounts. Similarly any temperature dependence in the empirical curves which is really caused by humidity changes which are correlated with temperature, may not represent the situation as well in a changed climate if the relation between temperature and humidity changes. Quantifying and/or reducing this source of uncertainty may be a worthwhile subject for future research.

3.2(i) Results for London

Table 6 shows the calculated rural background pollutant levels derived from the rural prediction for London and the predicted change between past and future years. These show an increase in ozone levels consistent with the increase in temperatures in the period 2071-2086 and decreases in NO_x consistent with the increased preponderance of westerlies advecting cleaner air into the area. By comparing the ranges in the values under the current and future climates with the differences in the means and by looking at the extent to which the ranges overlap, it seems highly likely that the changes in NO_x and ozone are significant while the changes in NO_2 and PM_{10} are not distinguishable from year-to-year variability.

Table 6. Annual average background values from the rural predictor - London

Year	Annual average			
	NO_x (ppb)	NO_2 (ppb)	O_3 (ppb)	PM_{10} (μg/m^3)
1971	18.77	8.18	24.28	17.19
1976	14.69	7.84	24.38	16.69
1981	14.82	7.07	25.10	16.94
1986	18.57	7.97	29.50	18.12
19xx average	16.71	7.77	25.81	17.23
2071	12.37	7.48	32.58	17.81
2076	12.65	7.34	31.46	17.63
2081	12.81	7.57	31.85	18.06
2086	11.97	7.06	27.94	17.18
20xx average	12.45	7.36	30.96	17.67
Change (%) 19xx to 20xx	**-25.5**	**-5.3**	**+20.0**	**+2.6**

Using the background values from the rural predictor, concentrations of NO_x, NO_2, PM_{10} and O_3 were predicted using the ADMS-Urban model for a set of receptor locations across London. The locations of these receptor points are given in Table 7.

Table 7. Receptor locations (UK National Grid) - London

Receptor	x (m)	y (m)	Height (m)
Marylebone Rd	528118	182017	3
Bloomsbury	530185	181955	3
Tower Hamlets	536105	182311	3
Lewisham	537679	173682	3
Southwark Bkg	532281	178470	15
Hackney	534839	186191	5
Haringey Roadside	533892	190645	3
Cromwell Road	526516	178966	2
N Kensington	524070	181691	3
Wandsworth	525829	174678	5
West London	524918	178846	30
Camden	526624	184393	3
Southwark Roadside	534619	177700	4
Bromley	540527	169328	2.5
Bexley	551850	176350	3
Eltham	543929	174564	2.5
Brent	519607	189342	3
Hounslow	517465	178042	2
A3	519270	165327	3
Teddington	515650	170650	15
Hillingdon	506977	178579	3
Sutton Suburban	527845	164686	3

The total annual average concentration predicted at each receptor location is given, for the four current climate years, in Table 8 and, for the four future climate years, in Table 9. The equivalent results with the contribution from the background concentration removed are given in Tables 10 and 11. Except for the case of O_3 this represents the contribution to concentration for local emissions. Note that as there are no emissions of O_3, the only contribution to O_3 is from the background, and indeed values are generally reduced below background by chemical processes. Hence, once the background concentration is removed, the resulting concentration of O_3 is negative. This has been included in the tables, however, to show the reduction in ozone due to local processes. Table 12 shows the concentrations (including background) averaged over the four current and four future climate years, together with the difference between the concentrations for the current and future climate. The equivalent results with the contribution from the background concentration removed are given in Table 13.

Table 12 shows that, between the current and future climates, concentrations of NO_x are predicted to decrease at all receptor locations. Conversely concentrations of NO_2 at most receptors are predicted to increase due to the increased background concentrations of O_3, shown in Table 6. Total concentrations of PM_{10} and O_3 are predicted to increase at virtually all receptor locations. However Table 13 (concentrations with background subtracted) shows that this increase is due to the increase in background concentrations. Without the contribution from the background, concentrations of PM_{10} and O_3 are predicted to decrease at all receptor locations.

Looking at the individual years in Tables 8-11 shows that the decrease in NO_x and the increase in O_3 are unlikely to be chance events due to our sample of years. For any one site, the ranges of the concentrations in the four current and four future years are often disjoint or showing only a small overlap. The same cannot be said for the increases in concentrations of NO_2 and PM_{10} where the ranges show significant overlap. In the case of NO_2, 1986 often shows the highest values of NO_2, despite the fact that generally values are higher in the future climate than the current one. This is almost certainly associated with the high background O_3 and NO_x in 1986 (see Table 6).

These tables show that the differences in predicted concentration are limited. From Tables 12 and 13, the maximum predicted changes when averaged across the four sample years in the current and future climates are as follows:

- The maximum predicted difference in NO_x concentrations, an average decrease of 11.5ppb, occurs at Marylebone Road. Without the background concentration, the maximum predicted difference in NO_x concentrations is a decrease of 7.3ppb, also at Marylebone Road.
- The maximum predicted difference in NO_2 concentrations, an average increase of 2.0ppb, occurs at Cromwell Road. Without the background concentration, the maximum predicted difference in NO_2 concentrations is an increase of 2.4ppb, also at Cromwell Road.
- The maximum predicted difference in PM_{10} concentrations, an average increase of 0.5µg/m^3, occurs at Bromley. Without the background concentration, the maximum predicted difference in PM_{10} concentrations is a decrease of 0.9µg/m^3 at Marylebone Road.
- The maximum predicted difference in O_3 concentrations, an average increase of 5.1ppb, occurs at Brent. Without the background concentration, the maximum predicted difference in O_3 concentrations is a decrease of 3.0ppb at Marylebone Road.

A summary of the results, averaged over all the sites, is given in Tables 14 and 15, with Table 15 showing results with the contribution from the background concentration removed. In summary the model predicts a decrease in NO_x, some increases in O_3 (arising from the increase in regional ozone due to the increase in temperature), little change in NO_2 (the increase in ozone being offset by the predicted decreases in NO_x), and little change in PM_{10}.

Table 8. Predicted annual average concentrations, 1971 - 1986 (London)

Receptor name	1971				1976				1981				1986			
	NO_x ppb	NO_2 ppb	PM_{10} ug/m^3	0_3 ppb	NO_x ppb	NO_2 ppb	PM_{10} ug/m^3	0_3 ppb	NO_x ppb	NO_2 ppb	PM_{10} ug/m^3	0_3 ppb	NO_x ppb	NO_2 ppb	PM_{10} ug/m^3	0_3 ppb
Marylebone Rd	147	39	32.1	5.7	142	39	31.5	5.8	133	37	30.7	6.8	157	45	34.2	6.3
Bloomsbury	62	28	21.6	8.8	57	27	21.0	8.5	53	26	20.8	10	65	31	22.8	11
Tower Hamlets	61	27	21.7	9.3	56	27	21.1	9.1	53	26	21.1	10	64	31	23.1	11
Lewisham	49	24	20.3	11	44	24	19.7	12	41	22	19.6	13	51	27	21.4	14
Southwark Bkg	46	24	20.1	11	41	24	19.5	11	39	23	19.5	12	48	27	21.2	14
Hackney	48	24	20.3	11	43	24	19.7	11	40	23	19.7	12	50	27	21.4	13
Haringey Roadside	52	25	21.8	10	48	25	21.3	10	45	24	21.1	11	55	29	23.1	12
Cromwell Road	99	33	26.1	7.2	95	33	25.5	7.0	88	31	25.0	8.1	105	38	27.6	8.2
N Kensington	45	24	20.2	11	40	23	19.6	11	38	22	19.5	12	47	26	21.3	14
Wandsworth	53	25	20.9	11	48	25	20.3	11	45	23	20.2	12	56	28	22.1	13
West London	45	24	20.0	11	40	23	19.4	11	38	22	19.4	12	47	26	21.1	14
Camden	72	29	22.5	8.5	69	29	22.1	8.4	64	27	21.9	10	76	33	23.9	10
Southwark Roadside	77	30	22.9	8.5	72	29	22.3	8.4	68	28	22.2	9.3	81	34	24.2	10
Bromley	48	23	19.9	12	44	23	19.4	12	42	22	19.5	13	50	27	21.0	14
Bexley	34	19	18.7	15	28	19	18.1	15	28	18	18.3	15	34	21	19.7	18
Eltham	35	20	18.9	14	30	20	18.3	14	29	19	18.4	15	36	22	19.9	17
Brent	31	19	18.7	15	27	18	18.2	15	26	17	18.3	16	33	20	19.8	19
Hounslow	52	24	20.1	12	47	24	19.5	12	44	22	19.5	13	55	27	21.3	14
A3	70	26	20.6	12	65	25	20.0	12	60	24	19.9	13	74	29	21.8	14
Teddington	30	17	18.3	16	25	17	17.8	16	24	16	17.9	17	31	19	19.4	20
Hillingdon	66	26	20.2	11	62	26	19.7	11	59	24	19.7	12	71	30	21.5	13
Sutton Suburban	31	18	18.5	16	26	18	18.0	16	25	16	18.0	17	32	19	19.6	19

Table 9. Predicted annual average concentrations, 2071 - 2086 (London)

Receptor name	2071				2076				2081				2086			
	NO_x ppb	NO_2 ppb	PM_{10} ug/m^3	0_3 ppb	NO_x ppb	NO_2 ppb	PM_{10} ug/m^3	0_3 ppb	NO_x ppb	NO_2 ppb	PM_{10} ug/m^3	0_3 ppb	NO_x ppb	NO_2 ppb	PM_{10} ug/m^3	0_3 ppb
Marylebone Rd	138	44	32.4	8.6	131	41	31.4	8.9	133	42	32.0	8.7	130	39	30.9	7.1
Bloomsbury	54	30	22.0	14	52	28	21.6	14	53	29	22.2	14	52	28	21.3	11
Tower Hamlets	54	30	22.3	14	52	28	21.8	14	53	29	22.4	14	53	28	21.6	11
Lewisham	41	25	20.7	18	40	24	20.4	17	40	25	20.9	17	39	24	20.0	14
Southwark Bkg	39	25	20.6	17	38	24	20.3	17	39	25	20.8	17	39	25	20.1	13
Hackney	40	26	20.8	17	38	25	20.4	17	40	25	20.9	17	38	24	20.0	13
Haringey Roadside	45	27	22.4	16	43	26	21.9	16	44	26	22.5	16	42	25	21.5	13
Cromwell Road	92	37	26.6	11	89	35	26.0	11	92	36	26.7	11	92	35	26.0	8.2
N Kensington	37	25	20.6	18	36	24	20.2	17	37	24	20.8	17	36	23	19.9	14
Wandsworth	45	27	21.4	17	44	25	21.0	16	45	26	21.5	16	44	25	20.6	13
West London	37	25	20.5	18	36	23	20.1	18	37	24	20.7	17	36	24	19.8	14
Camden	66	32	23.1	14	61	30	22.4	14	63	31	23.1	14	63	29	22.3	10
Southwark Roadside	70	33	23.4	13	67	31	22.9	13	68	32	23.5	13	69	31	22.8	10
Bromley	42	25	20.6	18	41	24	20.3	18	42	25	20.7	17	43	25	20.1	13
Bexley	26	20	19.2	22	26	19	18.9	21	26	20	19.4	21	27	19	18.7	17
Eltham	28	20	19.4	21	27	19	19.1	21	28	20	19.6	21	28	20	18.9	17
Brent	24	19	19.2	23	24	18	18.9	22	24	18	19.4	22	23	18	18.5	18
Hounslow	44	25	20.6	18	44	24	20.3	17	45	25	20.8	17	45	25	20.0	14
A3	61	28	21.0	17	59	26	20.7	17	60	27	21.2	17	55	25	20.1	14
Teddington	22	17	18.8	24	23	17	18.7	23	23	17	19.1	23	22	17	18.2	19
Hillingdon	59	28	20.8	16	55	26	20.3	17	56	27	20.8	17	54	25	19.9	14
Sutton Suburban	23	18	19.0	23	24	17	18.9	23	24	18	19.3	22	23	17	18.4	19

Table 10. Predicted annual average concentrations, 1971 - 1986, without background (London)

Receptor name	1971				1976				1981				1986			
	NO_x ppb	NO_2 ppb	PM_{10} ug/m^3	0_3 ppb	NO_x ppb	NO_2 ppb	PM_{10} ug/m^3	0_3 ppb	NO_x ppb	NO_2 ppb	PM_{10} ug/m^3	0_3 ppb	NO_x ppb	NO_2 ppb	PM_{10} ug/m^3	0_3 ppb
Marylebone Rd	128	31	14.9	-19	127	31	14.8	-19	119	30	13.8	-18	138	37	16.0	-23
Bloomsbury	43	19	4.4	-16	42	20	4.3	-16	38	19	3.9	-15	46	23	4.7	-19
Tower Hamlets	42	19	4.6	-15	41	19	4.5	-15	38	19	4.1	-15	46	23	4.9	-19
Lewisham	30	16	3.1	-13	29	16	3.0	-13	26	15	2.7	-13	32	19	3.3	-15
Southwark Bkg	27	16	2.9	-13	26	16	2.8	-13	24	16	2.6	-13	29	19	3.1	-16
Hackney	29	16	3.1	-13	29	16	3.0	-14	25	16	2.7	-13	31	19	3.3	-16
Haringey Roadside	34	17	4.7	-14	34	17	4.7	-14	30	17	4.2	-14	36	21	5.0	-17
Cromwell Road	81	25	8.9	-17	80	25	8.8	-17	73	24	8.0	-17	86	30	9.5	-21
N Kensington	27	15	3.0	-13	26	15	2.9	-13	23	15	2.6	-13	29	18	3.2	-16
Wandsworth	34	17	3.7	-14	34	17	3.6	-14	30	16	3.2	-13	37	20	4.0	-17
West London	26	15	2.8	-13	25	15	2.7	-13	23	15	2.4	-13	28	18	3.0	-15
Camden	53	21	5.4	-16	54	21	5.4	-16	50	20	4.9	-16	58	25	5.8	-19
Southwark Roadside	58	21	5.7	-16	58	22	5.6	-16	53	21	5.2	-16	63	26	6.1	-20
Bromley	29	15	2.7	-12	29	16	2.7	-13	28	15	2.5	-13	31	19	2.9	-15
Bexley	15	11	1.5	-10	14	11	1.4	-10	13	11	1.3	-10	15	13	1.6	-12
Eltham	16	12	1.7	-10	15	12	1.6	-10	15	12	1.5	-10	17	14	1.8	-12
Brent	13	10	1.5	-9.2	13	10	1.5	-9.2	11	10	1.3	-9.1	14	12	1.6	-11
Hounslow	33	16	2.9	-12	32	16	2.8	-13	29	15	2.5	-12	36	19	3.2	-15
A3	51	18	3.4	-13	51	17	3.3	-12	45	17	3.0	-12	56	21	3.7	-16
Teddington	11	9.3	1.1	-8.3	11	9.2	1.1	-8.2	9.0	8.6	0.9	-7.7	12	11	1.3	-10
Hillingdon	47	18	3.1	-13	47	18	3.0	-13	44	17	2.8	-13	52	22	3.4	-17
Sutton Suburban	12	10	1.3	-8.7	12	10	1.3	-8.6	10	9.2	1.1	-8.3	13	11	1.5	-10

Table 11. Predicted annual average concentrations, 2071 - 2086, without background (London)

Receptor name	2071				2076				2081				2086			
	NO_x ppb	NO_2 ppb	PM_{10} ug/m^3	0_3 ppb	NO_x ppb	NO_2 ppb	PM_{10} ug/m^3	0_3 ppb	NO_x ppb	NO_2 ppb	PM_{10} ug/m^3	0_3 ppb	NO_x ppb	NO_2 ppb	PM_{10} ug/m^3	0_3 ppb
Marylebone Rd	126	36	14.6	-24	118	34	13.8	-23	120	35	13.9	-23	118	32	13.8	-21
Bloomsbury	41	22	4.2	-18	39	21	4.0	-18	40	22	4.1	-18	40	21	4.1	-17
Tower Hamlets	41	22	4.5	-18	39	21	4.2	-17	40	22	4.3	-18	41	21	4.4	-17
Lewisham	28	18	2.9	-15	27	17	2.8	-14	28	17	2.8	-15	27	17	2.8	-14
Southwark Bkg	26	18	2.8	-15	25	17	2.7	-14	26	18	2.8	-15	27	18	2.9	-15
Hackney	28	18	3.0	-16	26	17	2.7	-15	27	18	2.9	-15	26	17	2.8	-15
Haringey Roadside	33	20	4.6	-16	31	19	4.3	-16	31	19	4.4	-16	30	18	4.3	-15
Cromwell Road	80	29	8.8	-22	76	28	8.4	-20	79	29	8.7	-21	80	28	8.8	-20
N Kensington	25	17	2.8	-15	23	16	2.6	-14	25	17	2.7	-15	24	16	2.7	-14
Wandsworth	33	19	3.5	-16	32	18	3.4	-15	32	19	3.5	-16	32	18	3.4	-15
West London	25	17	2.6	-15	24	16	2.5	-14	25	17	2.6	-15	24	17	2.6	-14
Camden	54	24	5.3	-19	48	22	4.8	-18	50	23	5.0	-18	51	22	5.1	-18
Southwark Roadside	57	25	5.6	-20	54	24	5.3	-18	55	25	5.4	-19	57	24	5.6	-18
Bromley	30	18	2.8	-15	28	17	2.6	-14	29	17	2.7	-14	31	18	2.9	-15
Bexley	14	12	1.4	-11	13	11	1.3	-10	13	12	1.4	-11	15	12	1.5	-11
Eltham	15	13	1.6	-11	15	12	1.5	-11	15	13	1.5	-11	16	13	1.7	-11
Brent	12	11	1.4	-10	11	10	1.3	-9.4	12	11	1.3	-10	11	11	1.4	-10
Hounslow	32	18	2.7	-15	31	17	2.7	-14	32	18	2.8	-15	33	17	2.8	-14
A3	48	20	3.2	-15	47	19	3.1	-14	47	20	3.1	-15	43	18	2.9	-14
Teddington	10	10	1.0	-8.7	10	9.3	1.0	-8.4	10	10	1.1	-9.0	10	10	1.0	-8.7
Hillingdon	47	21	3.0	-16	42	19	2.7	-15	43	19	2.8	-15	42	18	2.7	-14
Sutton Suburban	11	10	1.2	-9.2	11	10	1.3	-8.8	11	10	1.2	-9.4	11	10	1.2	-9.1

Table 12. Average predicted annual average concentrations by site (London)

Receptor name	19xx				20xx				Difference (20xx – 19xx)			
	NO_x ppb	NO_2 ppb	PM_{10} ug/m^3	0_3 ppb	NO_x ppb	NO_2 ppb	PM_{10} ug/m^3	0_3 ppb	NO_x ppb	NO_2 ppb	PM_{10} ug/m^3	0_3 ppb
Marylebone Rd	145	40	32.1	6.1	133	42	31.7	8.3	-11.5	1.8	-0.4	2.2
Bloomsbury	59	28	21.6	9.4	53	29	21.8	13	-6.4	0.9	0.2	3.6
Tower Hamlets	59	28	21.8	10	53	29	22.0	13	-5.8	0.9	0.3	3.7
Lewisham	46	24	20.3	12	40	24	20.5	17	-6.2	0.4	0.2	4.2
Southwark Bkg	43	24	20.1	12	39	25	20.5	16	-4.8	0.5	0.4	4.2
Hackney	45	25	20.3	12	39	25	20.5	16	-6.2	0.2	0.2	4.3
Haringey Roadside	50	26	21.9	11	44	26	22.1	15	-6.4	0.3	0.2	4.2
Cromwell Road	97	34	26.0	7.6	91	36	26.3	10	-5.5	2.0	0.3	2.6
N Kensington	43	24	20.2	12	37	24	20.4	17	-6.1	0.2	0.2	4.4
Wandsworth	51	25	20.9	11	45	26	21.1	15	-6.0	0.6	0.2	4.0
West London	42	24	20.0	12	37	24	20.3	17	-5.5	0.3	0.3	4.3
Camden	70	30	22.6	9.1	63	30	22.7	13	-7.2	0.8	0.1	3.7
Southwark Roadside	75	30	22.9	9.0	68	32	23.1	12	-6.4	1.4	0.2	3.1
Bromley	46	24	20.0	13	42	25	20.4	17	-4.0	0.7	0.5	4.0
Bexley	31	19	18.7	16	26	19	19.1	20	-4.7	-0.1	0.4	4.8
Eltham	33	20	18.9	15	28	20	19.3	20	-4.8	0.0	0.4	4.7
Brent	29	19	18.7	16	24	18	19.0	21	-5.4	-0.5	0.3	5.1
Hounslow	49	24	20.1	13	45	25	20.4	17	-4.8	0.8	0.4	3.9
A3	67	26	20.6	13	59	27	20.7	16	-8.7	0.5	0.2	3.8
Teddington	27	17	18.3	17	23	17	18.7	22	-4.9	-0.2	0.4	4.9
Hillingdon	64	26	20.3	12	56	26	20.4	16	-8.6	0.1	0.1	4.2
Sutton Suburban	28	18	18.5	17	24	18	18.9	22	-4.9	-0.2	0.4	4.9

Table 13. Average predicted annual average concentrations by site, without background (London)

Receptor name	19xx				20xx				Difference (20xx – 19xx)			
	NO_x ppb	NO_2 ppb	PM_{10} ug/m^3	0_3 ppb	NO_x ppb	NO_2 ppb	PM_{10} ug/m^3	0_3 ppb	NO_x ppb	NO_2 ppb	PM_{10} ug/m^3	0_3 ppb
Marylebone Rd	128	32	14.9	-20	121	34	14.0	-23	-7.3	2.2	-0.9	-3.0
Bloomsbury	42	20	4.3	-16	40	22	4.1	-18	-2.2	1.3	-0.2	-1.5
Tower Hamlets	42	20	4.5	-16	40	21	4.3	-18	-1.5	1.3	-0.2	-1.5
Lewisham	29	16	3.0	-13	27	17	2.8	-14	-1.9	0.8	-0.2	-1.0
Southwark Bkg	27	17	2.9	-14	26	17	2.8	-15	-0.5	0.9	-0.1	-1.0
Hackney	29	17	3.0	-14	27	18	2.8	-15	-2.0	0.6	-0.2	-0.8
Haringey Roadside	33	18	4.6	-15	31	19	4.4	-16	-2.1	0.7	-0.2	-0.9
Cromwell Road	80	26	8.8	-18	79	28	8.7	-21	-1.2	2.4	-0.2	-2.5
N Kensington	26	16	2.9	-14	24	17	2.7	-14	-1.8	0.6	-0.2	-0.8
Wandsworth	34	18	3.6	-14	32	19	3.5	-15	-1.8	1.0	-0.2	-1.1
West London	26	16	2.7	-14	24	17	2.6	-14	-1.3	0.7	-0.1	-0.8
Camden	54	22	5.4	-17	51	23	5.1	-18	-2.9	1.2	-0.3	-1.5
Southwark Roadside	58	23	5.7	-17	56	24	5.5	-19	-2.1	1.8	-0.2	-2.0
Bromley	29	16	2.7	-13	30	17	2.7	-14	0.2	1.1	0.0	-1.1
Bexley	14	12	1.4	-10	14	12	1.4	-11	-0.5	0.3	0.0	-0.4
Eltham	16	12	1.6	-11	15	13	1.6	-11	-0.5	0.4	0.0	-0.4
Brent	13	11	1.5	-10	11	11	1.3	-10	-1.2	0.0	-0.1	-0.1
Hounslow	33	16	2.8	-13	32	18	2.8	-14	-0.6	1.2	-0.1	-1.2
A3	51	18	3.3	-13	46	19	3.1	-15	-4.4	0.9	-0.3	-1.3
Teddington	11	9.4	1.1	-8.4	10	10	1.0	-8.7	-0.7	0.2	-0.1	-0.2
Hillingdon	48	19	3.1	-14	43	19	2.8	-15	-4.3	0.5	-0.3	-0.9
Sutton Suburban	12	10	1.3	-8.9	11	10	1.2	-9.1	-0.6	0.2	-0.1	-0.2

Table 14. Average predicted annual average concentrations across all sites (London)

Years	NO_x ppb	NO_2 ppb	PM_{10} ug/m^3	0_3 ppb
1971	57	25	21.1	11
1976	52	25	20.5	11
1981	49	23	20.5	12
1986	60	28	22.3	14
19xx average	**55**	**25**	**21.1**	**12**
19xx range	**49 to 60**	**23 to 28**	**20.5 to 22.3**	**11 to 14**
2071	49	27	21.6	17
2076	48	25	21.2	17
2081	49	26	21.7	17
2086	48	25	20.9	13
20xx average	**48**	**26**	**21.4**	**16**
20xx range	**48 to 49**	**25 to 27**	**20.9 to 21.7**	**13 to 17**
Average difference (20xx – 19xx)	**-6.1**	**0.5**	**0.3**	**4.0**

Table 15. Average predicted annual average concentrations across all sites with background subtracted (London)

Years	NO_x ppb	NO_2 ppb	PM_{10} ug/m^3	0_3 ppb
1971	38	17	3.9	-13
1976	38	17	3.9	-13
1981	34	16	3.5	-13
1986	41	20	4.2	-16
19xx average	**38**	**17**	**3.9**	**-14**
19xx range	**34 to 41**	**16 to 20**	**3.5 to 4.2**	**-16 to -13**
2071	37	19	3.8	-15
2076	35	18	3.6	-15
2081	36	19	3.7	-15
2086	36	18	3.7	-14
20xx average	**36**	**18**	**3.7**	**-15**
20xx range	**35 to 37**	**18 to 19**	**3.6 to 3.8**	**-15 to -14**
Average difference (20xx – 19xx)	**-1.9**	**0.9**	**-0.2**	**-1.1**

3.2(ii) Results for Glasgow

Table 16 shows the calculated rural background pollutant levels derived from the rural predictor for Glasgow and the predicted change between past and future years. These show an increase in ozone levels consistent with the increase in temperatures in the period 2071-2086 and a decrease in NO_X and NO_2. This is consistent with the results for London; however the changes in ozone and NO_X are much reduced compared with the changes predicted for London. The small change in PM_{10} is not significant given the strong overlap between the range of values in the individual years under the current climate and the future climate.

Table 16. Annual average background values from the rural predictor - Glasgow

Year	Annual average			
	NO_x (ppb)	NO_2 (ppb)	O_3 (ppb)	PM_{10} (µg/m³)
1971	7.34	5.85	27.16	16.55
1976	7.18	5.57	27.44	15.94
1981	6.88	5.16	27.77	16.18
1986	7.15	5.50	26.86	16.14
19xx average	7.14	5.52	27.31	16.20
2071	6.88	5.08	28.52	16.29
2076	6.86	5.04	28.37	16.41
2081	6.53	4.75	29.77	16.73
2086	6.67	4.78	28.72	15.78
20xx average	6.73	4.91	28.85	16.30
Change (%) 19xx to 20xx	**-5.7**	**-11.1**	**+5.6**	**+0.6**

Using the background values from the rural predictor, concentrations of NO_x, NO_2, PM_{10} and O_3 were predicted using ADMS-Urban for a set of receptor locations across Glasgow. The locations of these receptor points are given in Table 17.

Table 17. Receptor locations (UK National Grid) - Glasgow

Receptor	x (m)	y (m)	Height (m)
Glasgow Centre	258950	665054	0
City Chambers	259517	665346	0
Glasgow Kerbside	258688	665145	0
M8 J17-18	258363	666437	0
M8 J20-21	257150	664219	0
Alexandra Pd	261718	665499	0
Urban bgd S	259787	664374	0
Rural bgd SE	261663	663281	0
Urban bgd Centre	258242	665577	0
Rural bgd SW	256808	662961	0

As with the case for London the total annual average concentration predicted at each receptor location is given, for the four current climate years, in Table 18 and, for the four future climate years, in Table 19. The equivalent results with the contribution from the background concentration removed are given in Tables 20 and 21. Table 22 shows the concentrations (including background) averaged over the four current and four future climate years, together with the difference between the concentrations for the current and future climate. The equivalent results with the contribution from the background concentration removed are given in Table 23.

Table 22 shows small decreases in NO_x and NO_2 at most receptor locations, small increases in ozone, and a mixed picture for PM_{10}. However, looking at the individual years in Tables 18 and 19 it is clear that there is substantial overlap between the range of the concentrations in the four years under the current climate and the range under the future climate. As a result we cannot, with only 2 × four years of data available for this study, conclude that these changes are significant.

The tables show that the differences in predicted concentrations are quite small. From Tables 22 and 23, the maximum predicted changes when averaged across the four sample years in the current and future climates are as follows:

- The maximum predicted difference in NO_x concentrations, an average decrease of 3.1ppb, occurs at M8 J20-21. Without the background concentration, the maximum predicted difference in NO_x concentrations is a decrease of 2.7ppb, also at M8 J20-21.
- The maximum predicted difference in NO_2 concentrations, an average decrease of 0.8ppb, occurs at Rural bgd SW. Without the background concentration, the maximum predicted difference in NO_2 concentrations is an increase of 0.7ppb at Alexandra Pd.
- The maximum predicted difference in PM_{10} concentrations is 0.2µg/m³, occurring at three of the modelled receptor locations (M8 J20-21, Rural bgd SE and Urban bgd Centre). Without the background concentration, the maximum predicted difference in PM_{10} concentrations is a decrease of 0.3µg/m³ at M8 J20-21 and Urban bgd Centre.
- The maximum predicted difference in O_3 concentrations, an average increase of 1.5ppb, occurs at Rural bgd SW. Without the background concentration, the maximum predicted difference in O_3 concentrations is a decrease of 0.9ppb at M8 J17-18, M8 J20-21 and Alexandra Pd.

A summary of the results, averaged over all the sites, is given in Tables 24 and 25, with Table 25 showing results with the contribution from the background concentration removed. In summary the impacts of climate change on pollutant concentrations at Glasgow are predicted to be small. In fact the size of the changes are smaller than the year to year variability and, with the small number of years of data available to this study, it is unclear whether they are a consequence of our selection of years or of climate change.

Table 18. Predicted annual average concentrations, 1971 - 1986 (Glasgow)

Receptor name	1971				1976				1981				1986			
	NO_x ppb	NO_2 ppb	PM_{10} ug/m^3	0_3 ppb	NO_x ppb	NO_2 ppb	PM_{10} ug/m^3	0_3 ppb	NO_x ppb	NO_2 ppb	PM_{10} ug/m^3	0_3 ppb	NO_x ppb	NO_2 ppb	PM_{10} ug/m^3	0_3 ppb
Glasgow Centre	40	21	22.0	13	37	20	20.9	15	34	18	20.6	16	40	21	21.7	13
City Chambers	30	19	19.9	15	28	18	19.0	16	25	16	19.0	18	30	19	19.6	15
Glasgow Kerbside	44	22	22.5	13	41	21	21.3	14	37	19	21.0	16	45	22	22.1	13
M8 J17-18	68	25	22.1	13	63	24	21.0	14	58	22	20.8	15	67	25	21.7	13
M8 J20-21	75	27	23.2	11	69	26	22.0	12	63	24	21.7	13	75	27	22.8	11
Alexandra Pd	26	18	19.5	16	24	17	18.6	17	23	16	18.6	18	27	18	19.2	16
Urban bgd S	28	17	19.3	17	27	16	18.4	18	24	15	18.4	19	27	17	18.8	17
Rural bgd SE	17	14	18.8	20	16	13	18.0	21	15	12	18.1	21	18	14	18.6	19
Urban bgd Centre	50	23	23.0	13	46	22	21.8	14	41	20	21.3	15	50	23	22.6	12
Rural bgd SW	15	12	18.2	21	14	12	17.4	22	13	10	17.4	23	15	12	17.8	21

Table 19. Predicted annual average concentrations, 2071 - 2086 (Glasgow)

Receptor name	2071				2076				2081				2086			
	NO_x ppb	NO_2 ppb	PM_{10} ug/m^3	0_3 ppb	NO_x ppb	NO_2 ppb	PM_{10} ug/m^3	0_3 ppb	NO_x ppb	NO_2 ppb	PM_{10} ug/m^3	0_3 ppb	NO_x ppb	NO_2 ppb	PM_{10} ug/m^3	0_3 ppb
Glasgow Centre	37	21	21.4	14	36	20	21.3	15	36	20	21.6	16	35	19	20.5	15
City Chambers	28	18	19.5	17	27	18	19.5	17	26	17	19.8	18	26	17	18.8	17
Glasgow Kerbside	42	21	21.8	14	41	21	21.8	14	40	21	22.0	16	40	20	21.0	15
M8 J17-18	64	25	21.4	14	62	24	21.5	14	60	23	21.6	15	59	23	20.6	15
M8 J20-21	70	27	22.4	12	68	26	22.4	12	66	26	22.6	13	66	25	21.6	13
Alexandra Pd	26	17	19.2	17	25	17	19.2	17	25	17	19.5	18	24	17	18.5	18
Urban bgd S	27	17	18.8	18	26	16	18.8	18	25	16	19.1	19	24	15	18.1	19
Rural bgd SE	17	13	18.6	20	16	13	18.6	21	16	13	19.0	22	16	13	17.9	21
Urban bgd Centre	46	22	22.2	14	45	22	22.2	14	44	21	22.4	15	43	21	21.3	15
Rural bgd SW	14	11	17.7	23	14	11	17.8	22	13	11	18.1	24	13	10	17.1	23

Table 20. Predicted annual average concentrations, 1971 - 1986, without background (Glasgow)

Receptor name	1971				1976				1981				1986			
	NO_x ppb	NO_2 ppb	PM_{10} ug/m^3	0_3 ppb	NO_x ppb	NO_2 ppb	PM_{10} ug/m^3	0_3 ppb	NO_x ppb	NO_2 ppb	PM_{10} ug/m^3	0_3 ppb	NO_x ppb	NO_2 ppb	PM_{10} ug/m^3	0_3 ppb
Glasgow Centre	33	15	5.5	-14	30	14	5.0	-13	27	13	4.4	-12	33	16	5.5	-14
City Chambers	22	13	3.4	-12	20	12	3.1	-11	18	11	2.8	-10	23	13	3.5	-12
Glasgow Kerbside	37	16	5.9	-14	34	15	5.4	-13	31	14	4.8	-12	38	16	6.0	-14
M8 J17-18	61	19	5.6	-14	55	18	5.1	-13	51	17	4.6	-13	60	19	5.5	-14
M8 J20-21	68	22	6.6	-16	62	20	6.1	-15	56	19	5.5	-14	68	22	6.7	-16
Alexandra Pd	19	12	2.9	-11	17	11	2.7	-10	16	10	2.5	-10	20	12	3.1	-11
Urban bgd S	20	11	2.7	-10	20	11	2.5	-10	18	10	2.2	-8.7	20	12	2.7	-10
Rural bgd SE	10	7.8	2.2	-7.4	9.3	7.2	2.1	-6.9	8.6	6.8	1.9	-6.5	11	8.2	2.5	-7.7
Urban bgd Centre	42	17	6.4	-15	38	16	5.8	-14	34	15	5.2	-13	43	17	6.5	-15
Rural bgd SW	7.9	6.5	1.7	-6.2	7.1	5.9	1.4	-5.8	5.8	5.1	1.2	-5.0	8.2	6.7	1.7	-6.4

Table 21. Predicted annual average concentrations, 2071 - 2086, without background (Glasgow)

Receptor name	2071				2076				2081				2086			
	NO_x ppb	NO_2 ppb	PM_{10} ug/m^3	0_3 ppb	NO_x ppb	NO_2 ppb	PM_{10} ug/m^3	0_3 ppb	NO_x ppb	NO_2 ppb	PM_{10} ug/m^3	0_3 ppb	NO_x ppb	NO_2 ppb	PM_{10} ug/m^3	0_3 ppb
Glasgow Centre	31	16	5.1	-14	30	15	4.9	-14	29	15	4.8	-14	28	15	4.7	-13
City Chambers	21	13	3.2	-12	20	13	3.1	-12	20	12	3.1	-12	19	12	3.0	-11
Glasgow Kerbside	35	16	5.5	-14	34	16	5.4	-14	34	16	5.3	-14	33	15	5.2	-14
M8 J17-18	57	20	5.2	-15	56	19	5.0	-15	54	19	4.9	-15	53	18	4.8	-14
M8 J20-21	63	22	6.1	-17	62	21	6.0	-16	60	21	5.8	-16	59	21	5.8	-16
Alexandra Pd	19	12	2.9	-12	18	12	2.8	-11	18	12	2.8	-11	18	12	2.7	-11
Urban bgd S	20	12	2.5	-11	20	11	2.4	-10	19	11	2.4	-10	18	11	2.3	-10
Rural bgd SE	11	8.4	2.3	-8.1	10	7.7	2.2	-7.5	10	7.9	2.2	-7.8	10	8.0	2.2	-7.8
Urban bgd Centre	39	17	5.9	-15	38	17	5.8	-14	38	17	5.7	-15	36	16	5.5	-14
Rural bgd SW	6.6	6.0	1.4	-6.0	6.8	6.0	1.4	-6.0	6.6	5.9	1.4	-6.0	6.1	5.7	1.3	-5.7

Table 22. Average predicted annual average concentrations by site (Glasgow)

Receptor name	19xx				20xx				Difference (20xx – 19xx)			
	NO_x ppb	NO_2 ppb	PM_{10} ug/m^3	0_3 ppb	NO_x ppb	NO_2 ppb	PM_{10} ug/m^3	0_3 ppb	NO_x ppb	NO_2 ppb	PM_{10} ug/m^3	0_3 ppb
Glasgow Centre	38	20	21.3	14	36	20	21.2	15	-1.7	-0.3	-0.1	0.9
City Chambers	28	18	19.4	16	27	18	19.4	17	-1.3	-0.3	0.0	1.0
Glasgow Kerbside	42	21	21.7	14	41	21	21.6	15	-1.4	-0.2	-0.1	0.9
M8 J17-18	64	24	21.4	14	61	24	21.3	14	-2.6	-0.1	-0.1	0.7
M8 J20-21	71	26	22.4	12	67	26	22.3	13	-3.1	-0.1	-0.2	0.6
Alexandra Pd	25	17	19.0	17	25	17	19.1	18	-0.3	0.1	0.1	0.7
Urban bgd S	27	16	18.7	18	26	16	18.7	19	-0.9	-0.3	0.0	1.0
Rural bgd SE	17	13	18.4	20	17	13	18.5	21	-0.2	-0.1	0.2	0.9
Urban bgd Centre	47	22	22.2	13	45	22	22.0	14	-2.1	-0.3	-0.2	0.9
Rural bgd SW	14	12	17.7	21	13	11	17.7	23	-1.1	-0.8	0.0	1.5

Table 23. Average predicted annual average concentrations by site, without background (Glasgow)

Receptor name	19xx				20xx				Difference (20xx – 19xx)			
	NO_x ppb	NO_2 ppb	PM_{10} ug/m^3	0_3 ppb	NO_x ppb	NO_2 ppb	PM_{10} ug/m^3	0_3 ppb	NO_x ppb	NO_2 ppb	PM_{10} ug/m^3	0_3 ppb
Glasgow Centre	31	15	5.1	-13	29	15	4.9	-14	-1.3	0.3	-0.2	-0.6
City Chambers	21	12	3.2	-11	20	13	3.1	-12	-0.9	0.3	-0.1	-0.5
Glasgow Kerbside	35	15	5.5	-13	34	16	5.3	-14	-1.0	0.4	-0.2	-0.7
M8 J17-18	57	18	5.2	-14	55	19	5.0	-14	-2.2	0.5	-0.2	-0.9
M8 J20-21	63	21	6.2	-15	61	21	5.9	-16	-2.7	0.5	-0.3	-0.9
Alexandra Pd	18	11	2.8	-10	18	12	2.8	-11	0.1	0.7	0.0	-0.9
Urban bgd S	20	11	2.5	-10	19	11	2.4	-10	-0.4	0.3	-0.1	-0.6
Rural bgd SE	10	7.5	2.2	-7.1	10	8.0	2.2	-7.8	0.2	0.5	0.1	-0.7
Urban bgd Centre	39	16	6.0	-14	38	17	5.7	-14	-1.7	0.3	-0.3	-0.6
Rural bgd SW	7.3	6.1	1.5	-5.8	6.5	5.9	1.4	-5.9	-0.7	-0.2	-0.1	-0.1

Table 24. Average predicted annual average concentrations across all sites (Glasgow)

Years	NO_x ppb	NO_2 ppb	PM_{10} ug/m^3	0_3 ppb
1971	39	20	20.8	15
1976	37	19	19.9	16
1981	33	17	19.7	17
1986	40	20	20.5	15
19xx average	**37**	**19**	**20.2**	**16**
19xx range	**33 to 40**	**17 to 20**	**19.7 to 20.8**	**15 to 17**
2071	37	19	20.3	16
2076	36	19	20.3	16
2081	35	18	20.6	18
2086	35	18	19.5	17
20xx average	**36**	**19**	**20.2**	**17**
20xx range	**35 to 37**	**18 to 19**	**19.5 to 20.6**	**16 to 18**
Average difference (20xx – 19xx)	**-1.5**	**-0.2**	**0.0**	**0.9**

Table 25. Average predicted annual average concentrations across all sites with background subtracted (Glasgow)

Years	NO_x ppb	NO_2 ppb	PM_{10} ug/m^3	0_3 ppb
1971	32	14	4.3	-12
1976	29	13	3.9	-11
1981	26	12	3.5	-10
1986	33	14	4.4	-12
19xx average	**30**	**13**	**4.0**	**-11**
19xx range	**26 to 33**	**12 to 14**	**3.5 to 4.4**	**-12 to -10**
2071	30	14	4.0	-12
2076	29	14	3.9	-12
2081	29	14	3.8	-12
2086	28	13	3.7	-12
20xx average	**29**	**14**	**3.9**	**-12**
20xx range	**28 to 30**	**13 to 14**	**3.7 to 4.0**	**-12 to -12**
Average difference (20xx – 19xx)	**-1.1**	**+0.4**	**-0.1**	**-0.6**

3.3 Results from STOCHEM on Ozone Predictions and Climate Change

In this section we look at predictions of regional ozone obtained with a transport and chemical reaction model. This contrasts with the regional ozone predictions obtained using the statistical 'rural predictor' model presented in the last section. The model used is STOCHEM (Collins et al., 1997, Johnson et al., 2001), a global Lagrangian atmospheric chemistry model which is coupled to the Met Office's climate simulation models. The model represents the atmosphere using a large number of cells of equal mass that are moved through the atmosphere by the wind field. Each cell contains a chemical box model. In this study emissions are represented on a global longitude-latitude grid with 72 by 36 points and 50,000 cells are used, with each cell carrying around 50 species. Despite the fairly low resolution of this configuration of the model, it gives a good comparison with the seasonal cycle of ozone measured at Mace Head (Ireland), with a maximum in April and minimum in July/August. The model underpredicts the ozone slightly with a mean deviation of 2.7 ppb. The simulations available from this model use the SRES A2 scenario for emissions with the model coupled to the HadCM3 coupled atmosphere-ocean model. Results from two continuous simulations over the period 1990-2100 are presented, one with STOCHEM coupled to the control HadCM3 version, representing the pre-industrial climate and one with climate changes produced by HadCM3 in response to SRES A2 emissions. The fact that both these simulations take account of changes in anthropogenic emissions (but not changes in biogenic emissions) contrasts with the rural predictor ozone changes which only take direct account of meteorological changes, although there may be some accounting for biogenic emission changes to the extent that these are related to changes in meteorology (see discussion in Section 3.2).

Figure 31 shows the predicted ozone concentrations interpolated to London and Glasgow, and the mean concentration for the northern hemisphere, from the model coupled to the control HadCM3 version. Figure 32 shows the same data from the simulation where STOCHEM is coupled to the SRES A2 HadCM3 version. The data have been taken from the lowest model layer at approximately 950 mbar, and thus may overpredict surface ozone as the model vertical resolution is insufficient to account for shallow night time boundary layers where ozone becomes depleted due to dry deposition. Our experience shows that the model data is a good predictor of maximum daytime ozone within the constraints of its resolution. Both figures show the mean of the annual ozone cycle over the decades starting in 2000, 2030, 2060 and 2090, together with the minimum and maximum monthly mean within the decade for each month of the year. To clarify with an example, the April mean for the 2030 decade is the mean of the April values for 2030, 2031, …, 2039, while the April maximum for the 2030 decade is the maximum of these values. Table 26 shows a summary of the changes between the 2000 and 2090 decades. The decadal mean at both London and Glasgow increases between the 2000 and 2090 decades by about 14 ppb in the control simulation and 6 ppb in the climate change simulation. The change in the meteorology due to climate change has the effect of reducing the increase caused by the increase in emissions. We have also considered the peak monthly average over each decade (i.e. the ‘worst’ month in the decade). The increase in this quantity between the 2000 and 2090 decades is much larger than the increase in the mean, being of order 28 ppb in the control simulation and 14 ppb in the climate change simulation. This results in a peak monthly average in the 2090’s in excess of 60 ppb, even in the climate change simulation.

Table 26. Increases in ozone values (ppb) between the 2000-2009 and 2090-2099 decades as modelled by STOCHEM. Increases in the decadal mean and in the peak monthly average over the decade are shown.

Increase in:	Control meteorology		Climate change meteorology	
	London	Glasgow	London	Glasgow
Decadal mean	13.2	14.5	5.5	6.4
Peak monthly average	27.2	28.4	12.5	15.3

The negative effect of climate change on the ozone increases described above is consistent with the hypothesis that water vapour increases from climate change act generally to reduce ozone on large scales (Johnson et al., 1999). (Locally the effect of water vapour on ozone chemistry can be mixed with enhancements to both production and destruction processes.) Other factors which were not included in the simulations described above and could affect ozone concentrations are: 1) a potential increase in the amount of stratospheric ozone entering the troposphere due to recovery of stratospheric ozone and to an increase in the ozone flux across the tropopause (Zeng and Pyle, 2003; Butchart and Scaife, 2001; Collins et al., 2003) and 2) an increase in the natural emissions of hydrocarbons with temperature which is likely to lead to increased ozone (Sanderson et al., 2003), although different hydrocarbons have different effects (isoprene tends to increase ozone while terpenes tend to decrease ozone). Further studies are needed to clarify the net effect of these processes.

This analysis of STOCHEM results has only looked at monthly means. More extreme values are likely within the months, and the effect of climate change could increase this, especially if the frequency/duration of blocking weather patterns increases. We cannot address this with the existing data, but more detailed daily output could be obtained from future STOCHEM runs to address this issue. It would also be possible to run with interactive isoprene emissions to include the effect of these increasing with temperature. Also of interest would be simulations where the climate changes but the anthropogenic emissions are held at the pre-industrial levels, with and without interactive natural hydrocarbon emissions. This would help to determine whether the 'rural predictor' statistical approach is consistent with STOCHEM, and the extent to which it accounts implicitly for changes in natural hydrocarbon emissions driven by climate change.

(a)

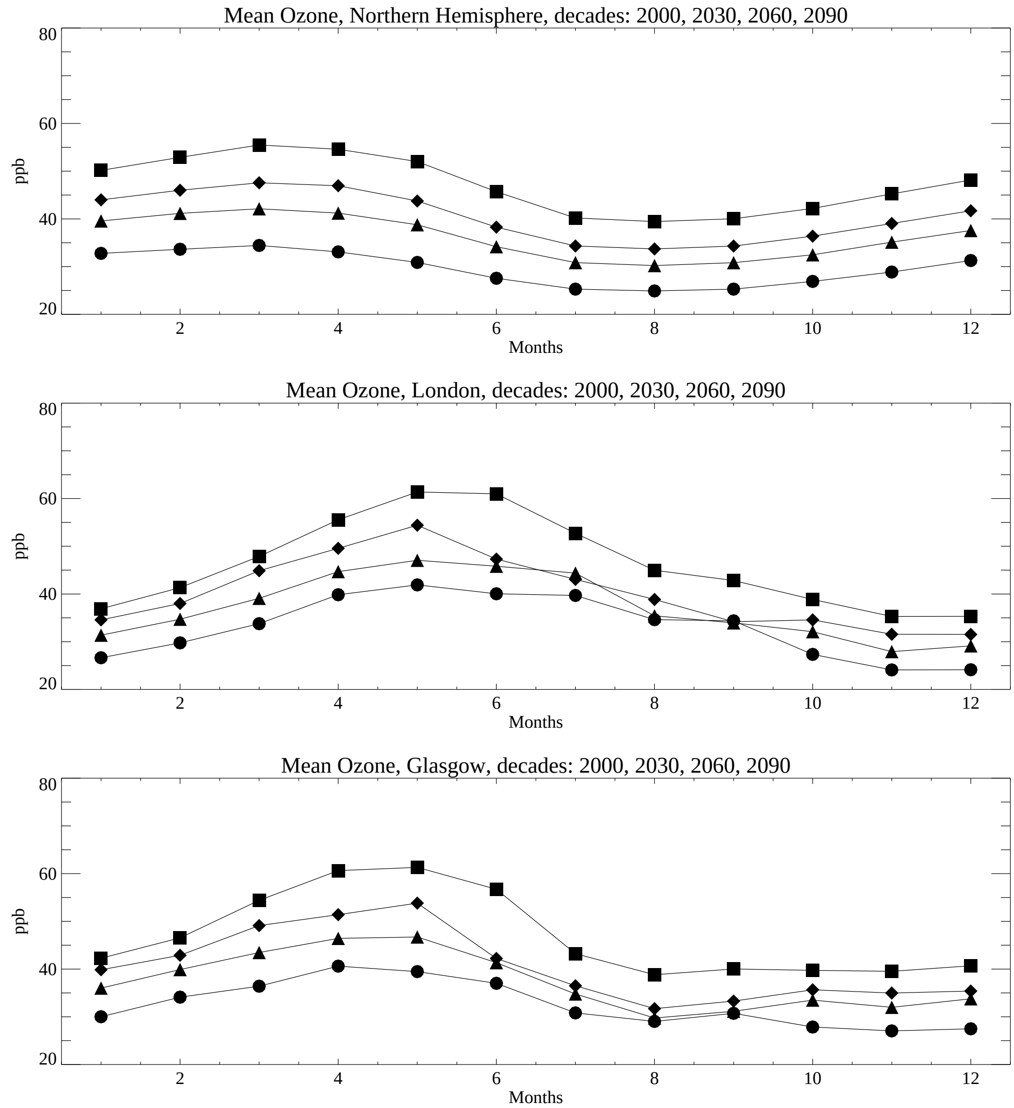

Figure 31: Ozone predictions from STOCHEM using SRES A2 emisions and the control meteorological climatology, for two locations (London and Glasgow) and averaged over the northern hemisphere. Monthly averages have been calculated and the mean, max and min of these values for each month of the year over a decade are plotted. (a), (b) and (c) show the mean, max and min respectively. Circles, triangles, diamonds and squares show results for decades starting in 2000, 2030, 2060 and 2090 respectively.

(b)

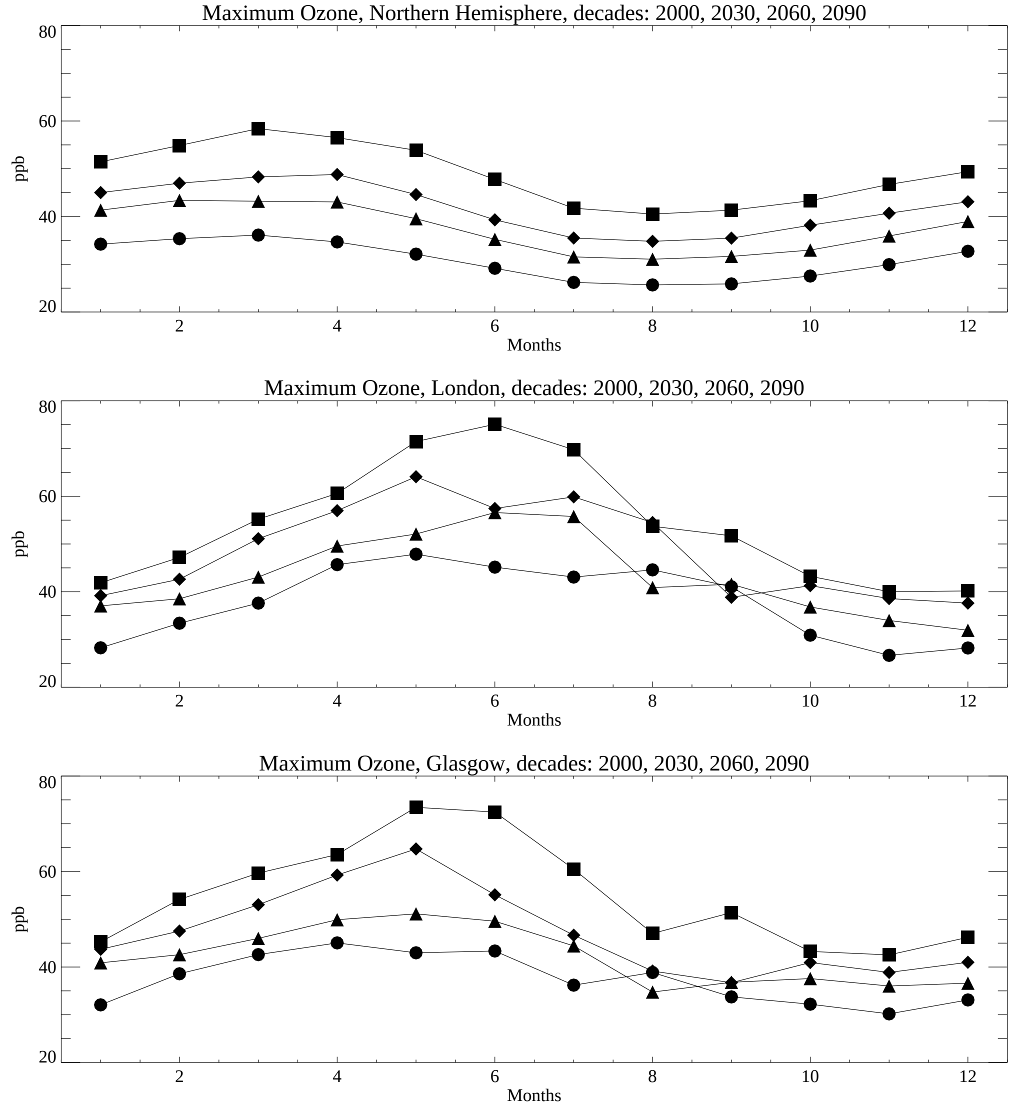

Figure 31 continued.

(c)

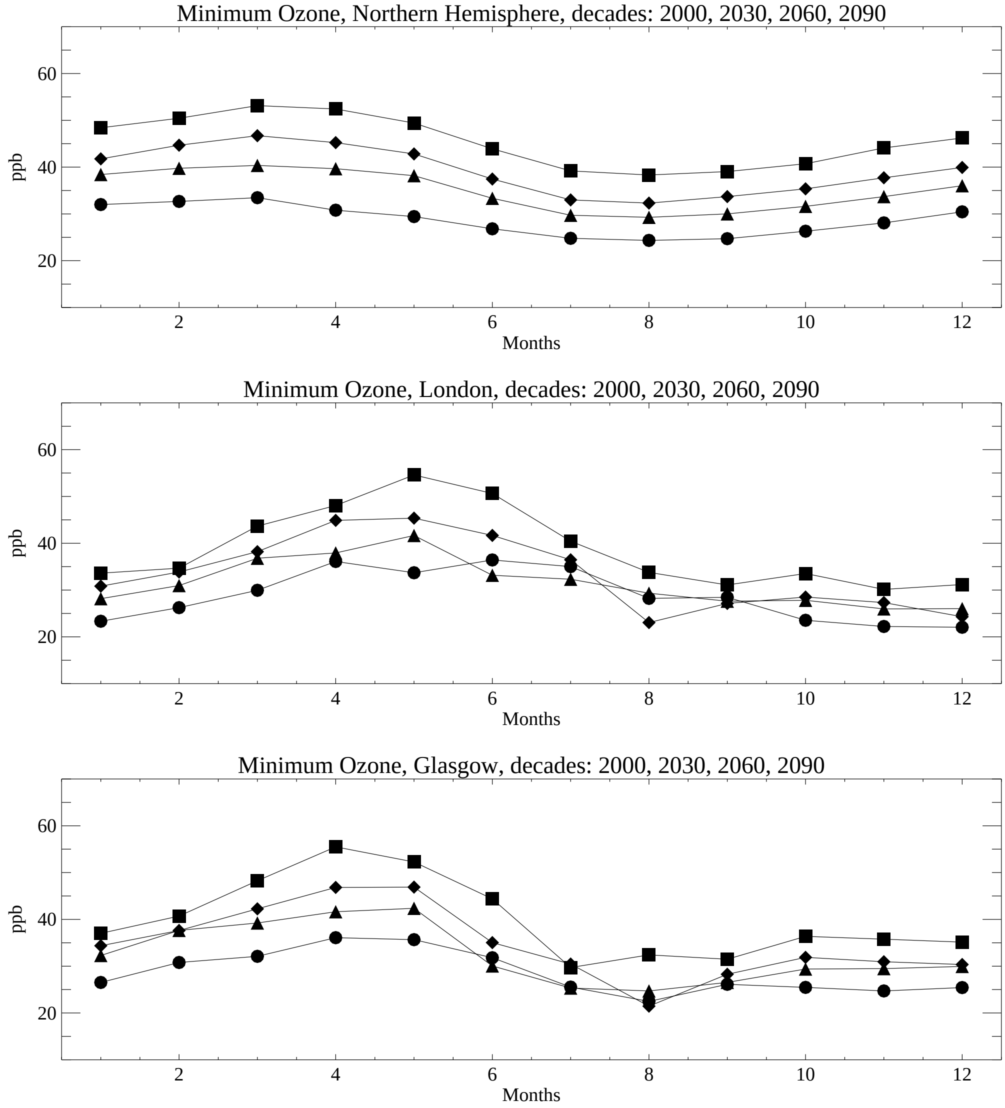

Figure 31 continued.

(a)

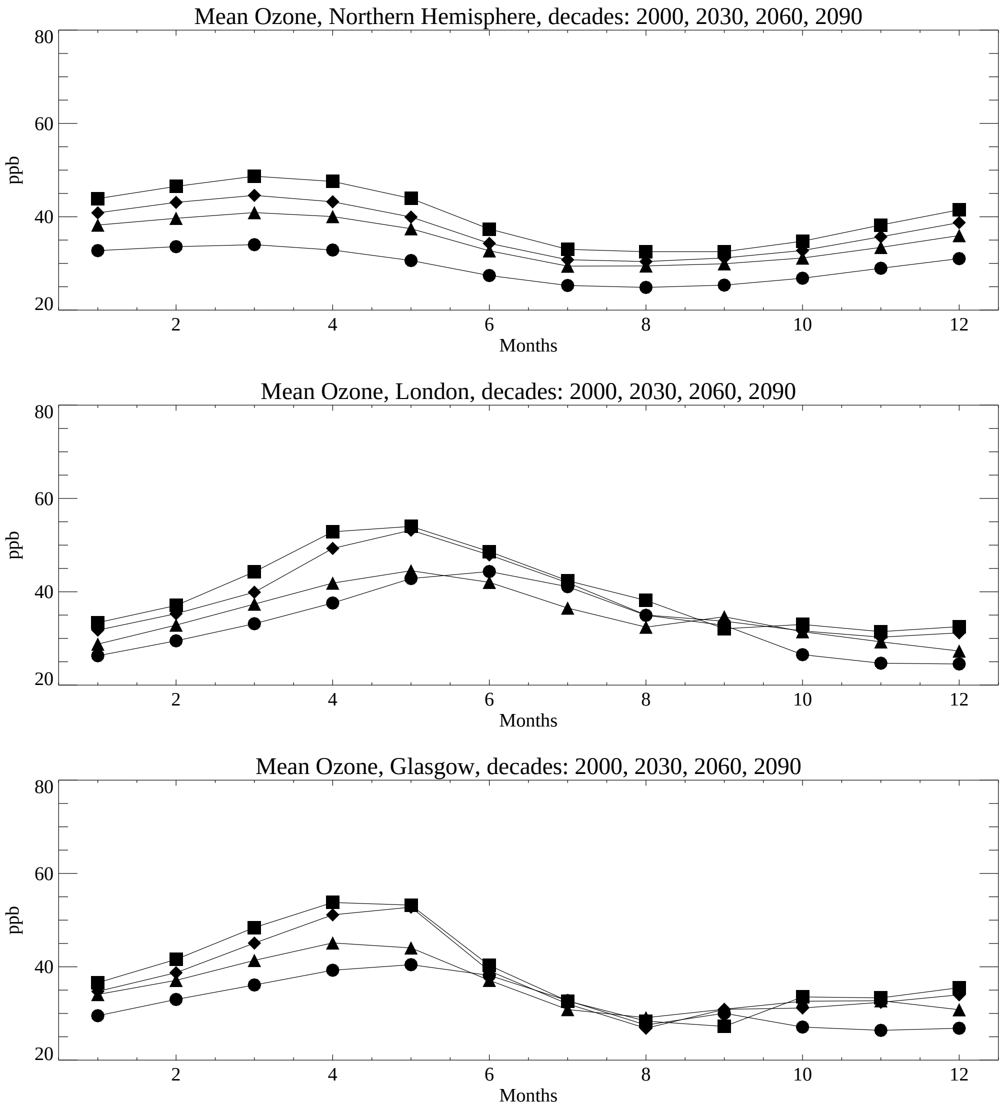

Figure 32: As Figure 31, but with the meteorological climatology changing in response to the SRES A2 emission scenario.

(b)

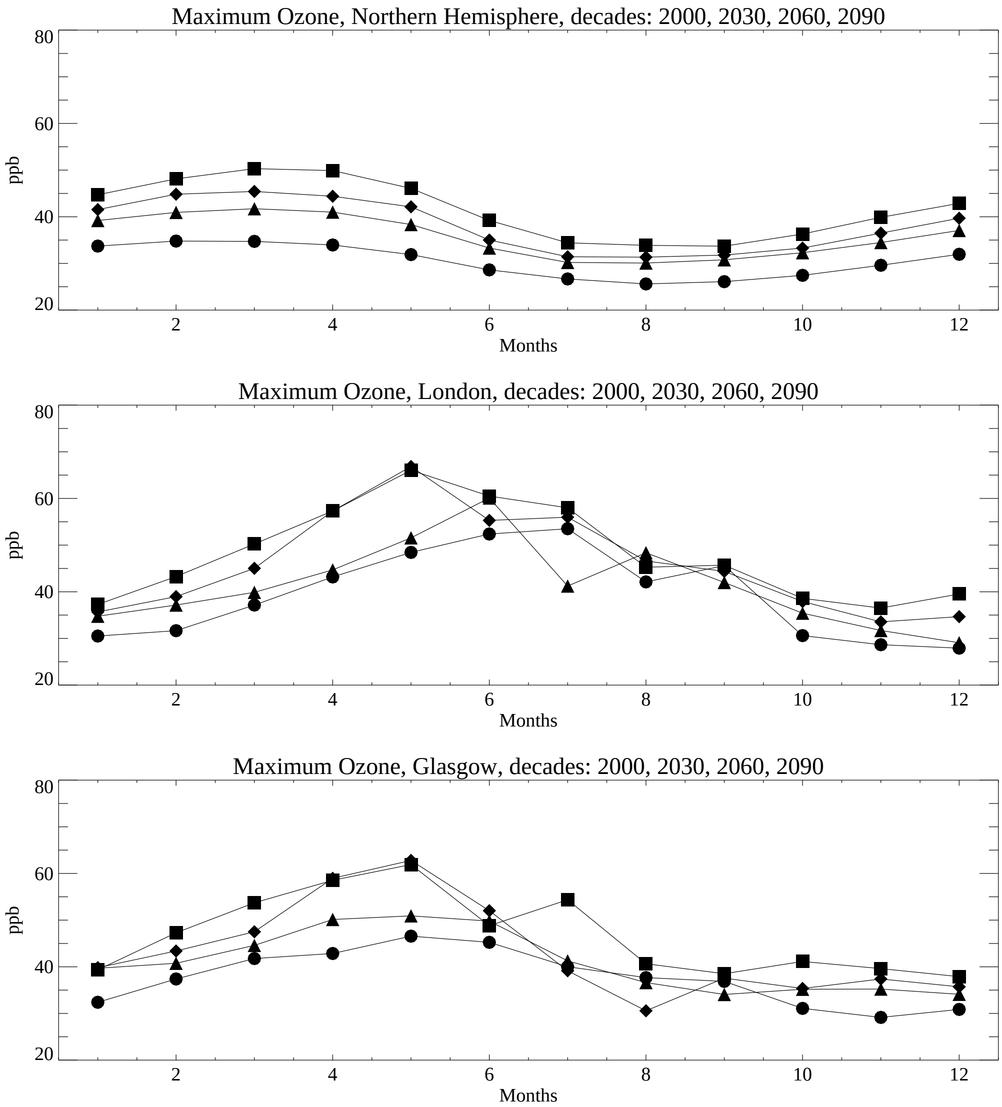

Figure 32 continued.

(c)

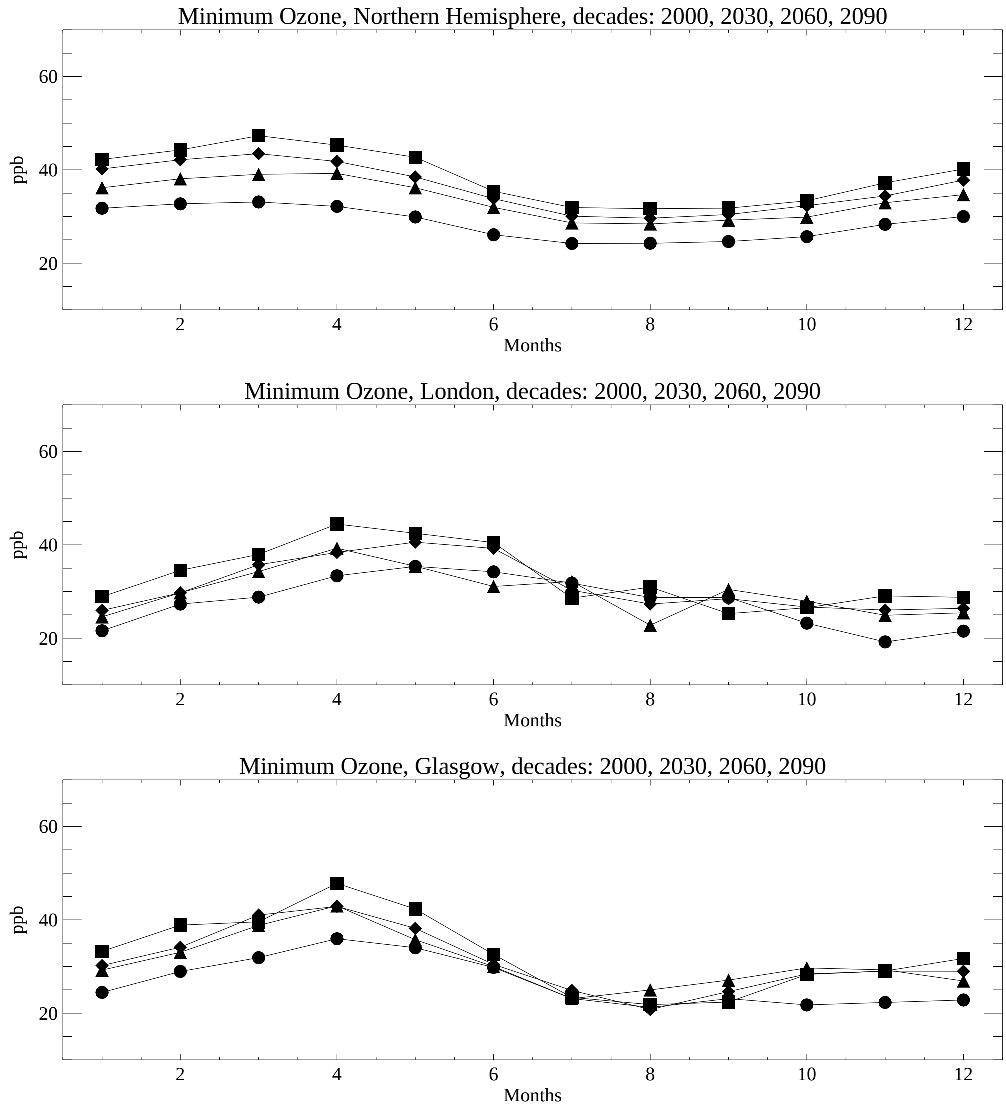

Figure 32 continued.

4. Conclusions

Meteorology from climate change simulations has been extracted for London and Glasgow. This has been used to estimate the impact of climate change on air quality in these two urban areas, using the statistical 'rural predictor' model to represent the regional background concentrations. Finally the results from an alternative approach to estimating regional background ozone concentrations, namely the use of the global chemical transport model 'STOCHEM', have been presented.

The climate change simulations have been used to predict changes between the current climate and a future climate in the period ~2070-2090. The most obvious impact of climate change is on temperature, with smaller and less clearly significant changes in other parameters. Increases of order 2-4 ^{0}C are predicted. This is a significant parameter for air pollution because of its effect, particularly in summer, on emission of biogenic ozone precursors and its influence on chemical reaction rates. Other changes with potential impacts on air quality are as follows:

- **Wind speed:** Increases in winter and reductions in summer are predicted at both locations. The main effect is likely to be a change in pollutant dilution at its source, although there will also be some changes through the consequent changes in stability.
- **Wind direction:** In London there is a tendency for more westerlies in winter and a shift from south-westerlies to north-westerlies in summer. In Glasgow there is a tendency for wind directions to become much more concentrated in the WSW direction. For Glasgow this is likely to lead to the impacts from large point sources being more concentrated in one sector, and hence higher. More generally the wind direction will influence the extent to which polluted air from Europe or cleaner air from the Atlantic is present. Hence the changes in wind direction suggest London should be cleaner in winter and Glasgow should be cleaner all year round, all else being equal.
- **Cloud cover:** This shows a small reduction in summer at both sites, and a modest consequential increase in incoming solar radiation (increasing photochemical production of ozone) and surface heat flux (increasing the ability of the boundary layer to disperse pollutants, but bringing pollutants from elevated sources to the ground more rapidly). There is little change in winter.
- **Boundary layer depth:** This is influenced by wind speed, surface heat flux and lapse rate above the boundary layer and shows a modest mean increase in London (~50m) and a very small mean increase in Glasgow (~10m). Increasing boundary layer depth has a similar effect to increased surface heat flux, increasing the dispersive ability of the boundary layer.
- **Precipitation:** This decreases in summer and increases in winter at both sites, and is relevant to air quality because of the ability of precipitation to wash out pollutants.
- **Mean sea level pressure:** This is not directly relevant to air quality, but is related to the type of circulation pattern and so has some relation with the other variables considered here and with factors not addressed by these variables such as the degree of boundary layer venting by convective clouds. It is predicted to become higher in summer and lower in winter, suggesting an increase in blocking circulation patterns in summer and in mobile westerly patterns in winter.
- **Specific humidity:** This is predicted to increase at both sites. It plays a significant role in ozone chemistry, and can enhance both production and destruction of ozone.

It must be pointed out that many aspects of climate change science are uncertain and so there are significant uncertainties in the above conclusions. These uncertainties are discussed in some detail by Hulme et al. (2002). With the present state of knowledge, the changes, especially of some of the more detailed boundary layer properties, must be regarded as indicative only. Results for temperature and winter precipitation are likely to be the most reliable with some degree of consensus between different models; summer precipitation and wind climatology are less reliable, varying significantly between different climate change models; while detailed boundary layer properties such as heat flux and boundary layer depth have not to our knowledge been subject to much scrutiny in terms of inter-model comparisons. In this study we have an extra source of uncertainty due to the fact that we have used only four years of data for representing the current climate and four years for the future climate. However for most of our conclusions on dispersion and air quality, the differences are either significantly larger than the year to year variability and so unlikely to be affected by this statistical problem or small enough not to be of concern.

Dispersion predictions were made for a variety of single sources: a small source with a low stack, a small power station, a large power station and a road source. With the London met data, only the large power station showed significant differences, with a 13% increase in the spatial maxima of the annual average and the 98th percentile concentrations by ~2080. For Glasgow the effects were larger with increases in the range 25-39% for the annual average for all three non-road sources and for the 98th percentile for the power station source.

Predictions for long term average background concentrations of NO_x, NO_2, ozone and PM_{10} upwind of London and Glasgow were made using the 'rural predictor' model. This showed a 4.3 ppb fall in NO_x and a 5.1 ppb increase in ozone for London, while a 0.6 ppb fall in NO_2 was the largest predicted percentage change (-11%) for Glasgow (again by about 2080). Other changes were small (of order 5% or less). Predictions of background ozone were also made with the STOCHEM chemical transport model. These simulations include increases in anthropogenic emissions corresponding to the A2 SRES scenario which are not allowed for in the rural predictor model. Predictions of a 6 ppb increase in long term average ozone are obtained, with similar values at both London and Glasgow. Although the rural predictor and STOCHEM give similar values for ozone (at least in London) it is important to realise that (i) the rural predictor does not account for the projected increase in anthropogenic emissions, and (ii) the version of STOCHEM used here does not account for the likely increase with temperature of natural biogenic hydrocarbon emissions. It seems possible that a model that includes both these aspects will result in higher ozone predictions. STOCHEM predicts larger increases in peak monthly mean concentrations of ozone, with the worst months having concentrations above 60 ppb.

With the aid of the background estimates from the rural predictor, long term average concentrations of NO_x, NO_2, ozone and PM_{10} were estimated within the two urban areas. For London the results averaged over a number of sites show a fall in NO_x of 6.1 ppb and a rise in ozone of 4.0 ppb with only small changes in NO_2 and PM_{10}. For Glasgow, the changes in all four chemical species are small. Bigger changes are seen at individual sites, e.g. a fall of 11.5 ppb in NO_x at Marylebone Road and an increase of 5.1 ppb in ozone at Brent.

This work has some implications from a policy perspective. Firstly the increases in impacts seen for some of the single sources imply that climate change may be important in the regulation of large sources. Increases in some concentration statistics of up to 40% seem possible in some situations. Secondly the impact of climate change on both rural and urban ozone may well be significant with increases of order 5 ppb. Peak increases could well be substantially higher. Ozone directives and standards are generally given in terms of 1 or 8 hr mean values. This means that it's difficult to directly compare a monthly or annual average to the standards. However, ozone exceedance statistics (see the Air Quality Archive at http://www.airquality.co.uk/archive/data_and_statistics.php) show that current UK air quality standards and objectives are presently exceeded at some sites at certain times. Any future increase in ozone due to climate change, such as that predicted in this study, would therefore be expected to produce more frequent exceedances of the UK and EC standards. This would have important consequences for the UK's ability to meet EC ozone directives (e.g. the third daughter directive). Also of significance is the fact that in London average NO_2 concentrations remain approximately constant despite reductions in NO_x. This results from greater availability of ozone and shows that projections of NO_2 based only on reductions of NO_x may underestimate NO_2.

All figures given in this report relate to the changes expected by about the year 2080. As a rough rule of thumb we recommend using the factors suggested by Hulme et al. (2002, p 43, table 7) in order to relate these predictions to other times. This means we expect 27% of the changes to occur by the 2020s and 57% by the 2050s. Of course there is no compelling reason to expect air quality changes to change in the same way as other climate impacts and this should be regarded as no more than a rough estimate in the absence of anything better.

It must be appreciated that there are many uncertainties in these figures and that quantifying and reducing this uncertainty will require further research. Indeed the figures should be regarded as no more than indicative of the actual outcome. Improvements in the ability to describe the climate change itself will occur as part of the world-wide climate change research effort. However there is an argument that, for air quality purposes, more attention should be given to boundary layer properties, boundary layer ventilation and air mass origins in climate change studies. Air mass origin information would be better than the single-location wind direction data used here in assessing whether polluted air from Europe or cleaner air from the Atlantic is present. In addition research aimed at improving our predictions of background concentrations would be welcome, e.g. for developing an understanding of the extent to which the rural predictor model will need to be changed to model the changed climate or through the development of chemical transport models to provide background estimates which include more processes and give results with finer time and space resolution. Where the changes are most significant, namely the NO_x and ozone predictions for London, the changes in urban concentrations are, averaged over the urban sites, very similar to the background changes, suggesting that future research on this topic should put more weight on the problem of predicting the background than the detailed urban chemistry. A detailed understanding of the urban chemistry is still needed however for site specific predictions. Future research should also put more emphasis on predictions of pollution episodes and extremes than has been possible in this short study.

5. References

Buonomo, E., D. Hassell and R. Jones, Report on impact of enhanced resolution on RCM simulations of present and future climate over the UK and Europe, Report to DEFRA from Hadley Centre for Climate Prediction and Research, Met Office, Exeter, UK, 2003.

Butchart, N. and A.A. Scaife, Removal of chlorofluorocarbons by increased mass exchange between the stratosphere and troposphere in a changing climate, Nature, **410**, 799-802, 2001.

Cambridge Environmental Research Consultants Ltd, The Advantages of ADMS, 2001. Available from http://www.cerc.co.uk/software/publications.htm

Carruthers, D.J., R.J. Holroyd, J.C.R. Hunt, W-S. Weng, A.G. Robins, D.D. Apsley, D.J. Thomson and F.B. Smith, UK-ADMS: A new approach to modelling dispersion in the earth's atmospheric boundary layer, Journal of Wind Engineering and Industrial Aerodynamics, **52**, 139-153, 1994.

Collins, W.J., D.S. Stevenson, C.E. Johnson, and R.G. Derwent, Tropospheric ozone in a global scale 3-D Lagrangian model and its response to NOx emission controls, J. Atmos Chem., **26**, 223-274, 1997.

Collins, W.J., R.G. Derwent, B. Garnier, C.E. Johnson, M.G. Sanderson and D.S. Stevenson, The effect of stratosphere-troposphere exchange on the future tropospheric ozone trend, J. Geophys. Res., **108,** doi 10.1029/2002JD002617, 2003.

Davies, B.M. and D.J. Thomson, Investigating the importance of pre-processing in estimating dispersion climatology, Int. J. Environment and Pollution, **8**, 590-603, 1997.

Dentener, F., D. Stevenson, K. Ellingsen, T. van Noije, M. Schultz, M. Amann, C. Atherton, N. Bell, D. Bergmann, I. Bey, L. Bouwman, T. Butler, J. Cofala, B. Collins, J. Drevet, R. Doherty, B. Eickhout, H. Eskes, A. Fiore, M. Gauss, D. Hauglustaine, L. Horowitz, I. Isaksen, B. Josse, M. Lawrence, M. Krol, J.F. Lamarque, V. Montanaro, J.F. Müller, V.H. Peuch, G. Pitari, J. Pyle, S. Rast, J. Rodriguez, M. Sanderson, N.H. Savage, D. Shindell, S. Strahan, S. Szopa, K. Sudo, R. Van Dingenen, O. Wild, G. Zeng., The global atmospheric environment for the next generation, submitted to Geophys. Res. Lettrs., 2005.

Frei, C., J.H. Christensen, M. Déqué, D. Jacob, R.G. Jones, P.L. Vidale, Daily precipitation statistics in regional climate models: Evaluation and intercomparison for the European Alps, J. Geophys. Res., **108**, 4124, doi 10.1029/2002JD002287, 2003.

Giorgi, F. and L.O. Mearns, Introduction to special section: Regional climate modeling revisited, J. Geophys. Res., **104**, 6335-6352, 1999.

Gordon, C., C. Cooper, C.A. Senior, H. Banks, J.M. Gregory, T.C. Johns, J.F.B. Mitchell, and R.A. Wood, The simulation of SST, sea ice extents and ocean heat transports in a version of the Hadley Centre coupled model without flux adjustments, Clim. Dyn., **16**, 147-168, 2000.

Hudson, D.A., and R.G. Jones, Simulations of present-day and future climate over southern Africa using HadAM3H, Tech. Note 38, Met Office Hadley Centre, Exeter, UK, 2002a.

Hudson, D.A. and R.G. Jones, Regional climate model simulations of present-day and future climates of southern Africa, Tech. Note 39, Met Office Hadley Centre, Exeter, UK, 2002b.

Hulme, M., G.J. Jenkins, X. Lu, J.R. Turnpenny, T.D. Mitchell, R.G. Jones, J. Lowe, J.M. Murphy, D. Hassell, P. Boorman, R. McDonald, and S. Hill, Climate change scenarios for the United Kingdom: The UKCIP02 Scientific Report, Tyndall Centre for Climate Change Research, School of Environmental Sciences, University of East Anglia, Norwich, UK, 2002.

Jenkins, G.J., C. Cooper, D.C. Hassell, R.G. Jones, Scenarios of climate change for islands within the BIC region, British-Irish Council Report, 2003. Available from http://www3.british-irishcouncil.org/climatechange/.

Johnson, C.E., W.J. Collins, D.S. Stevenson and R.G. Derwent, Relative roles of climate and emission changes on future tropospheric oxidant concentrations, J. Geophys. Res., **104**, 18631-18645, 1999.

Johnson, C.E., D.S. Stevenson, W.J. Collins and R.G. Derwent, Role of climate feedback on methane and ozone studied with a coupled Ocean-Atmosphere model, Geophys. Res. Lettrs., **28**, 1723-1726, 2001.

Jones, R.G., M. Noguer, D.C. Hassell, D. Hudson, S.S. Wilson, G.J. Jenkins and J.F.B. Mitchell, Generating high resolution climate change scenarios using PRECIS, Met Office Hadley Centre, Exeter, UK, 2004

Langner, J., R. Bergström and V. Foltescu, Impact of climate change on surface ozone and deposition of sulphur and nitrogen in Europe, Atmos. Environ., **39**, 1129, 2005

Lowe, J.A., J.M. Gregory and R.A. Flather, Changes in the occurrence of storm surges around the United Kingdom under a future climate scenario using a dynamic storm surge model driven by the Hadley Centre climate models, Climate Dynamics, **18**, 179-188, 2001.

Mattai, J., London Atmospheric Emissions Inventory 2001 (LAEI 2001), LAEI 2001 User Guide, 2003.

McHugh, C.A., D.J. Carruthers, and H.A. Edmunds, ADMS-Urban: an air quality management system for traffic, domestic and industrial pollution, Int. J. Environment and Pollution, **8**, 666-675, 1997.

Mickley, L.J., D.J. Jacob, B.D. Field and D. Rind, Effects of future climate change on regional air pollution episodes in the United States, Geophys. Res. Lettrs., **31**, doi 10.1029/2004GL021216, 2004.

Nakićenović, N., J. Alcamo, G. Davis, B. de Vries, J. Fenhann, S. Gaffin, K. Gregory, A. Grűbler, T.Y. Jung, T. Kram, E.L. La Rovere, L. Michaelis, S. Mori, T. Morita, W. Pepper, H. Pitcher, L. Price, K. Riahi, A. Roehrl, H.-H. Rogner, A. Sankovski, M. Schlesinger, P. Shukla, S. Smith, R. Swart, S. van Rooijen, N. Victor and Z. Dadi, Special report on emission scenarios: A special report of Working Group III of the Intergovernmental Panel on Climate Change, 2000.

Sanderson, M.G., C.D. Jones, W.J. Collins, C.E. Johnson and R.G. Derwent, Effect of climate change on isoprene emissions and surface ozone levels, Geophys. Res. Lettrs., **30**, doi 10.1029/2003GRL017642, 2003.

Zeng, G. and J.A. Pyle, Changes in tropospheric ozone between 2000 and 2100 modeled in a chemistry-climate model, Geophys. Res. Lettrs., **30**, 1392, doi:10.1029/2002/GL016708, 2003.